

AD-A124 450

CRYSTAL STRUCTURE AND EXCITED TRIPLET STATE ELECTRON  
PARAMAGNETIC RESONAN. (U) NORTH CAROLINA UNIV AT CHAPEL  
HILL DEPT OF CHEMISTRY S K HOFFMAN ET AL. 20 JAN 83

1/1

**UNCLASSIFIED**

TR-20 N00014-76-C-0816

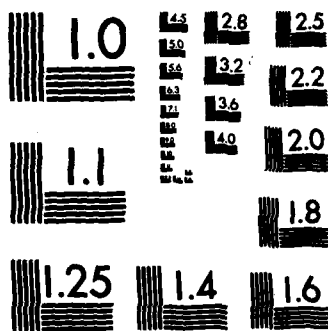
F/G 7/3

NL

END

FILMED

● ● ●



MICROCOPY RESOLUTION TEST CHART  
NATIONAL BUREAU OF STANDARDS-1963-A

13

SECURITY CLASSIFICATION OF THIS PAGE (When Data Entered)

REPORT DOCUMENTATION PAGE		READ INSTRUCTIONS BEFORE COMPLETING FORM
1. REPORT NUMBER 20	2. GOVT ACCESSION NO. A124450	3. RECIPIENT'S CATALOG NUMBER
4. TITLE (and Subtitle) Crystal Structure and Excited Triplet State Electron Paramagnetic Resonance of the Sigma Bonded TCNQ Dimer in Bis-2,9-Dimethyl-1,10-Phenanthrolinecopper(I) Tetracyanoquinodimethane, [Cu(DMP) <sub>2</sub> ] <sub>2</sub> [TCNQ] <sub>2</sub>		5. TYPE OF REPORT & PERIOD COVERED Technical Report, Interim
7. AUTHOR(s) Stanislaw K. Hoffmann, Peter J. Corvan, Phirtu Singh, C.N. Sethulekshmi, Robert M. Metzger and William E. Hatfield		6. PERFORMING ORG. REPORT NUMBER
9. PERFORMING ORGANIZATION NAME AND ADDRESS Department of Chemistry 045A University of North Carolina Chapel Hill, North Carolina 27514		8. CONTRACT OR GRANT NUMBER(s) N00014-76-C-0816
11. CONTROLLING OFFICE NAME AND ADDRESS Office of Naval Research Department of the Navy Arlington, Virginia 22217		10. PROGRAM ELEMENT, PROJECT, TASK AREA & WORK UNIT NUMBERS
MONITORING AGENCY NAME & ADDRESS (if different from Controlling Office) Office of Naval Research Department of the Navy Arlington, Virginia 22217		12. REPORT DATE January 20, 1982
DISTRIBUTION STATEMENT (of this Report) Approved for Public Release, Distribution Unlimited		13. NUMBER OF PAGES 67
DISTRIBUTION STATEMENT (of the abstract entered in Block 20, if different from Report) This document has been approved for public release and sale; its distribution is unlimited.		15. SECURITY CLASS. (of this report) Unclassified
SUPPLEMENTARY NOTES To be published in JOURNAL OF THE AMERICAN CHEMICAL SOCIETY		15a. DECLASSIFICATION/DOWNGRADING SCHEDULE
19. KEY WORDS (Continue on reverse side if necessary and identify by block number) copper coordination compound      tetracyanoquinodimethanide salt crystal structure      electron paramagnetic resonance      excitons radical anions      Frenkel excitons		
20. ABSTRACT (Continue on reverse side if necessary and identify by block number) Reaction of bis-2,9-dimethyl-1,10-phenanthrolinecopper(I) iodide, [Cu(DMP) <sub>2</sub> I], with lithium tetracyanoquinodimethanide, LiTCNQ, yields the compound [Cu(DMP) <sub>2</sub> ] <sub>2</sub> [TCNQ] <sub>2</sub> , which crystallizes in the triclinic system space group P1 with lattice parameters a = 12.784, b = 13.400, c = 12.136 Å, α = 113.51°, β = 112.58°, and γ = 62.80°. The structure of the compound was solved by Fourier methods and refined by least squares techniques to R = 0.060 based on 1957 observed reflections. The structure consists of [Cu(DMP) <sub>2</sub> ] <sup>+</sup> cations and exocyclically sigma-bonded [TCNQ] <sub>2</sub> <sup>2-</sup> dimers.		

ADA 124450

DTIC FILE COPY

DTIC  
ELECTE  
FEB 16 1983  
S  
D  
E

DD FORM 1473 EDITION OF 1 NOV 65 IS OBSOLETE

88 02 015 076

SECURITY CLASSIFICATION OF THIS PAGE (When Data Entered)

## 20. Abstract

The carbon-carbon bond in the dimer is  $1.630(13)\text{\AA}$ , and the  $[\text{TCNQ}]_2^{2-}$  dimeric ions are arranged in linear chains along the  $[\bar{1}10]$  direction. Single crystal electron paramagnetic resonance studies have been carried out in the temperature range 300 to 490 K, and thermally activated triplet state ( $S = 1$ ) EPR spectra as well as doublet state ( $S = 1/2$ ) EPR spectra have been detected and thoroughly characterized. The data show that strongly localized triplet excitons on  $[\text{TCNQ}]_2^{2-}$  anions (self-trapped Frenkel excitons) give rise to triplet state EPR spectra with zero-field splitting parameters  $|D/hc| = 0.0111\text{ cm}^{-1}$  and  $|E/hc| = 0.0015\text{ cm}^{-1}$ . Theoretical calculations of the dipolar splitting indicate that the electronic and molecular structure of the excited state of the  $[\text{TCNQ}]_2^{2-}$  dimeric anion is best characterized by two distorted  $\text{TCNQ}^-$  anions with a distorted distribution of spin densities. An EPR signal at  $g = 2.0025$  has been attributed to isolated  $\text{TCNQ}^-$  radical anions. The activation energies for the triplet excitons (which corresponds to the breaking of the  $\sigma$ -bond) and for the isolated  $\text{TCNQ}^-$  radical anions are 0.55 and 0.24 eV, respectively.

Accession For	
NTIS GRA&I	<input checked="" type="checkbox"/>
DTIC TAB	<input type="checkbox"/>
Unannounced	<input type="checkbox"/>
Justification	
By	
Distribution/	
Availability Codes	
Avail and/or	
Dist	Special
A	



OFFICE OF NAVAL RESEARCH

Contract N00014-76-C-0816

Task No. NR 053-617

TECHNICAL REPORT NO. 20

CRYSTAL STRUCTURE AND EXCITED TRIPLET STATE ELECTRON  
PARAMAGNETIC RESONANCE OF THE SIGMA BONDED TCNQ DIMER IN  
BIS-2,9-DIMETHYL-1,10-PHENANTHROLINECOPPER(I)  
TETRACYANOQUINODIMETHANE  $[\text{Cu}(\text{DMP})_2]_2[\text{TCNQ}]_2$

by

Stanislaw K. Hoffmann, Peter J. Corvan, Phirtu Singh  
C. N. Sethulekshmi, Robert M. Metzger,  
and William E. Hatfield

Prepared for publication  
in  
JOURNAL OF THE AMERICAN CHEMICAL SOCIETY

January 20, 1983

Reproduction in whole or in part is permitted for any  
purpose of the United States Government.

This document has been approved for public release and  
sale; its distribution is unlimited.

Crystal Structure and Excited Triplet State Electron  
Paramagnetic Resonance of the Sigma Bonded TCNQ Dimer in  
Bis-2,9-Dimethyl-1,10-Phenanthrolinecopper(I)  
Tetracyanoquinodimethane,  $[\text{Cu}(\text{DMP})_2]_2[\text{TCNQ}]_2$

BY STANISLAW K. HOFFMANN,<sup>1a</sup> PETER J. CORVAN,<sup>1b</sup> PHIRTU SINGH,<sup>1</sup>  
C. N. SETHULEKSHMI,<sup>1</sup> ROBERT M. METZGER,<sup>2</sup>  
AND WILLIAM E. HATFIELD<sup>1\*</sup>

Contribution from the Department of Chemistry  
the University of North Carolina at Chapel Hill  
Chapel Hill, North Carolina 27514  
and the University of Mississippi  
University, Mississippi 38677

ABSTRACT

Reaction of bis-2,9-dimethyl-1,10-phenanthrolinecopper(I) iodide,  $[\text{Cu}(\text{DMP})_2\text{I}]$ , with lithium tetracyanoquinodimethanide,  $\text{LiTCNQ}$ , yields the compound  $[\text{Cu}(\text{DMP})_2]_2[\text{TCNQ}]_2$  which crystallizes in the triclinic system space group  $P\bar{1}$  with lattice parameters  $a = 12.784$ ,  $b = 13.400$ ,  $c = 12.136$  Å,  $\alpha = 113.51^\circ$ ,

$\beta = 112.58^\circ$ , and  $\gamma = 62.80^\circ$ . The structure of the compound was solved by Fourier methods and refined by least squares techniques to  $R = 0.060$  based on 1957 observed reflections. The structure consists of  $[\text{Cu}(\text{DMP})_2]^+$  cations and exocyclically sigma-bonded  $[\text{TCNQ}]_2^{2-}$  dimers. The carbon-carbon bond in the dimer is  $1.630(13) \text{ \AA}$ , and the  $[\text{TCNQ}]_2^{2-}$  dimeric ions are arranged in linear chains along the  $[\bar{1}10]$  direction. Single crystal electron paramagnetic resonance studies have been carried out in the temperature range 300 to 490 K, and thermally activated triplet state ( $S = 1$ ) EPR spectra as well as doublet state ( $S = 1/2$ ) EPR spectra have been detected and thoroughly characterized. The data show that strongly localized triplet excitons on  $[\text{TCNQ}]_2^{2-}$  anions (self-trapped Frenkel excitons) give rise to triplet state EPR spectra with zero-field splitting parameters  $|D/hc| = 0.0111 \text{ cm}^{-1}$  and  $|E/hc| = 0.0015 \text{ cm}^{-1}$ . Theoretical calculations of the dipolar splitting indicate that the electronic and molecular structure of the excited state of the  $[\text{TCNQ}]_2^{2-}$  dimeric anion is best characterized by two distorted  $\text{TCNQ}^-$  anions with a distorted distribution of spin densities. An EPR signal at  $g = 2.0025$  has been attributed to isolated  $\text{TCNQ}^-$  radical anions. The activation energies for the triplet excitons (which corresponds to the breaking of the  $\sigma$ -bond) and for the isolated  $\text{TCNQ}^-$  radical anions are 0.55 and 0.24 eV, respectively.

## INTRODUCTION

Crystals of many salts of TCNQ<sup>-</sup> exhibit highly anisotropic physical properties.<sup>3-7</sup> TCNQ is a strong electron acceptor and occurs principally as the radical anion TCNQ<sup>-</sup> or as weakly  $\pi$ -bonded dimers which often stack to form quasi-linear anionic chains. Often the linear chains are segregated and are uniformly or alternately spaced stacks of TCNQ<sup>-</sup> anions which are sometimes interspersed with neutral TCNQ molecules. Frequently, highly anisotropic electrical conductivities are observed with the highest electrical conductivity coinciding with the chain propagation direction. The diffusion or hopping of electrons along the chain gives rise to a motional averaging of EPR lines, and usually very narrow lines are observed ( $\Delta B_{pp} \approx 0.1$  G, 1.0 G = 0.1 mTesla). These may exhibit anomalous angular dependencies of linewidths near the chain or stack axes.<sup>8,9</sup>

There also exist weakly conductive crystals (conductivity below  $10^{-9} \Omega^{-1} \text{ cm}^{-1}$ ) of TCNQ salts in which transport mechanisms are not effective.<sup>10</sup> Usually the TCNQ moieties are not stacked in these latter, weakly conductive crystals, although dimer formation may still occur. In addition to the usual  $\pi$ -bonded dimers there are reports of two compounds which exhibit dimer formation through an unusually long, exocyclic, aliphatic carbon-carbon sigma bond.<sup>11,12</sup> These unusual dimers are found in  $[\text{Pt}(2,2'\text{-bpy})_2][\text{TCNQ}]_2$ <sup>11</sup> and in  $(\text{NEP})_2[\text{TCNQ}]_2$  (NEP is N-ethylphenazinium).<sup>12</sup> The magnetic properties of these



compounds are very interesting. EPR doublets of thermally activated triplet states have been observed in single crystal samples. Analogous EPR spectra have also been detected in  $\pi$ -bonded dimers<sup>13-17</sup>, trimers<sup>13,15,18</sup>, and tetramers.<sup>15,19-21</sup>

A phase transition to a paramagnetic phase has been observed for  $[\text{Pt}(\text{bpy})_2][\text{TCNQ}]_2$ .<sup>11,22</sup> The absence of hyperfine structure on the thermally activated EPR doublets indicates that the triplet excitons are not localized on TCNQ. This unusual behavior of the EPR in TCNQ crystals has been described in terms of thermally activated Frenkel<sup>17</sup> or Wannier<sup>8</sup> excitons, in terms of the Hubbard Hamiltonian,<sup>23</sup> and by a theoretical band treatment.<sup>24</sup>

Here, we report the synthesis of bis-[2,9-dimethyl-1,10-phenanthrolinecopper(I)][TCNQ]<sub>2</sub>, a compound which contains a  $\sigma$ -bonded  $[\text{TCNQ}]_2^{2-}$  dimer. The compound has been characterized by an X-ray crystal structure determination, and results of studies on thermally activated EPR signals in powdered and single crystal samples are also analyzed and reported.

#### EXPERIMENTAL

Synthesis- The compound  $[\text{Cu}(\text{DMP})_2]_2[\text{TCNQ}]_2$  was prepared from  $\text{Cu}(\text{DMP})_2\text{I}$ <sup>25</sup> and LiTCNQ. To 0.6 g  $\text{Cu}(\text{DMP})_2\text{I}$  in 100 mL methanol was added a solution of 0.209 g LiTCNQ in 50 mL methanol. The mixture was stirred for 30 minutes and the

rust-brown precipitate was collected by filtration, washed with 5 mL cold methanol, and air dried (yield 0.605 g). Small rust-brown crystals were obtained by recrystallization of the product from 300 mL hot acetone. As shown in Figure 1, the crystals grow as plate-like prisms elongated in the [001] direction with the largest crystal plane being ( $\bar{2}10$ ). Analysis: Calcd for  $\text{Cu}(\text{DMP})_2(\text{TCNQ})$ ,  $\text{C}_{40}\text{H}_{28}\text{N}_8\text{Cu}$ : C, 70.21; H, 4.12; N, 16.38. Found: C, 69.92; H, 4.01; N, 16.20.

X-Ray Crystallographic Studies- A crystal of approximate dimensions 0.35 x 0.25 x 0.10 mm was mounted on an eucentric goniometer head and was used for measuring cell-dimensions and intensities at 292 K on an Enraf-Nonius CAD-4 computer controlled diffractometer equipped with a molybdenum X-ray tube and a graphite monochromator. The cell constants were determined by a least squares refinement of the setting angles of 25 high angle reflections. The cell constants and other crystallographic data are given in Table I.

The intensities were rather weak; only 1957 reflections with intensities greater than  $3\sigma$  were observed out of a total of 4500 collected up to  $\theta = 27.5^\circ$ . These were corrected for background, and by a Lorentz and polarization factor but were not corrected for absorption. The linear absorption coefficient for  $\text{MoK}\alpha$  radiation is  $7.1 \text{ cm}^{-1}$ , which is quite small. All calculations were performed with the CAD-4 SDP set of programs on a PDP 11/34 computer, except for the drawings which were

performed on an IBM/370 computer using ORTEP-II.<sup>26</sup>

Structure Refinement- The copper atom was located from an origin removed Patterson synthesis and the rest of the atoms by successive difference Fourier syntheses, except for the methyl hydrogens which could not be located. The TCNQ moiety, however, was thought to be making an exceptionally short contact with its centrosymmetric counterpart. Specifically, C(38) (which has two cyano groups attached to it) was only 1.63 Å away from C(38'), the latter being in an adjacent TCNQ moiety. It was concluded that these two atoms may be covalently bound, and a bond angle calculation around C(38) immediately showed that the four atoms attached to C(38) were approximately tetrahedrally disposed. This confirmed the conclusion that a dimerization of TCNQ had occurred through the formation of an exocyclic, aliphatic, carbon-carbon  $\sigma$ -bond.

The refinement of the structure by full matrix least squares methods proceeded quite smoothly to a final conventional R-index of 0.060 and a weighted R-index of 0.070. Refinement in the non-centrosymmetric space group,  $P1$ , was not attempted since the size of the problem would have been too large not only for the computer programs, but also for the amount of intensity data available. However, the thermal parameters were well behaved, the final difference Fourier was quite clean (vide infra), and the inter- and intra-molecular distances, except for the C(38)-C(38') distance, were all normal. Considering the quality of the data, the space group  $P\bar{1}$  was assumed to be correct.

The function minimized was  $\sum w [|\underline{F}_O| - |\underline{F}_C|]^2$ . The weights  $w$  were taken to be  $4\underline{F}_O^2/\sigma(\underline{F}_O)^2$ . All atoms except hydrogens were refined with anisotropic thermal parameters; the hydrogens were refined isotropically. All parameters shifts in the last cycle of the refinement were less than  $1.0\sigma$ . The final difference Fourier showed no peak greater than  $0.2 e^-$ . The final positional parameters are listed in Table II, and the thermal parameters are deposited as Supplementary Material.

Electron Paramagnetic Resonance Measurements- EPR spectra of powdered and single crystal samples of  $[\text{Cu}(\text{DMP})_2]_2[\text{TCNQ}]_2$  were recorded with a Varian E-109 spectrometer using a rectangular  $\text{TE}_{102}$  cavity operating at about 9.17 GHz. The magnetic field was calibrated by means of a Walker-Magnion G-502 NMR gaussmeter and a Hewlett-Packard 5245L frequency counter.

The sensitivity of the spectrometer was calibrated by using a Varian weak-pitch sample and, independently, using a DPPH single crystal ( $1.275 \times 10^{21}$  spins/g). Comparison of the results of the calibration measurements indicates that the number of spins in a sample can be estimated with an accuracy of  $\pm 50\%$ . Relative changes of the unpaired spins concentrations with temperature can be determined, however, with much higher accuracy (about 0.5%).

The temperature dependences of the EPR spectra were measured in the temperature range 300 K to 490 K using an E-4557 Varian variable temperature accessory. The microwave cavity was thermally stabilized by a flux of cooling water. Temperatures

were measured with a copper-constantan thermocouple.

Crystals suitable for EPR measurements were very small ( $2 \times 0.6 \times 0.1$ ) mm plate-like prisms. The angular variation measurements were made in the 1,2,3 orthogonal reference system related to the  $(\bar{2}10)$  plane as shown in Figure 1. The axis designated 1 is perpendicular to the plane, and the 3-axis coincides with the crystallographic  $c$ -axis. An optical microscope with a simulated EPR goniometer system was used for accurate alignment of the crystal prior to measurements.

## RESULTS

Description of the Structure- The structure is not as accurate as we would have liked, mainly because of the paucity and the weakness of the intensity data. The nominal estimated standard deviations, as obtained from the least squares matrix, are approximately 0.013 Å in the C-C and C-N bond distances, and  $1.0^\circ$  in the bond angles involving C and N atoms.

An ORTEP<sup>26</sup> drawing of the TCNQ dimer is given in Figure 2, which shows that the TCNQ radical anion has indeed dimerized, the dimer bond distance, C(38)-C(38'), being 1.630(13) Å. This value is comparable to the values 1.631(4) Å<sup>11</sup> and 1.65(2) Å<sup>27</sup> reported previously for this distance in  $\sigma$ -bonded TCNQ dimers. Other bonds to C(38) have also lengthened substantially compared to the similar bonds at the terminal ends of the dimeric moiety. The bond angles at C(38), as shown in Figure 2, are essentially

tetrahedral. The dihedral angle between the six-atom ring of TCNQ and the five-atom  $C(CN)_2$  plane at the dimerization end is  $48^\circ$ , whereas that at the terminal end is only  $13^\circ$ .

A drawing of the  $[Cu^I(DMP)_2]^+$  cation with the atom numbering system is shown in Figure 3. The mean bond distances and angles in the DMP-moiety, assuming a  $C_{2v}$  molecular symmetry, are shown in Figure 4. The distances involving the copper atom are shown on Figure 3. The geometry around the copper atom is essentially tetrahedral, as expected for four-coordinate copper(I) complexes. The distortion from tetrahedral geometry results from the N---N chelate bite of the phenanthroline ligand which restricts two of the N-Cu-N angles at  $82.3^\circ$  and  $83.4^\circ$ . The other four N-Cu-N angles range from  $120.3^\circ$  to  $129.1^\circ$ . Each DMP-moiety forms a short and a long bond to the copper atom, the short bonds being 2.038 and 2.041 Å, and the long bonds being 2.082 and 2.093 Å. The two DMP-moieties in the  $[Cu(DMP)_2]^+$  cation are approximately perpendicular to each other, the dihedral angle being  $97.1^\circ$ .

There is no interaction between the  $[Cu(DMP)_2]^+$  cation and the  $[TCNQ]_2^{2-}$  anion except via normal van der Waals separations. One DMP moiety makes an angle of  $26.4^\circ$  and the other an angle of  $60.4^\circ$  with the  $[TCNQ]_2^{2-}$  dimer. The latter has its dimer bond close to the  $b$ -axis with its center located at  $(0,0,1/2)$  as shown in the stereo-diagram in Figure 5. The copper atom and one of the DMP moieties and their centrosymmetrically related counterparts occupy the region around the origin of the cell.

The  $[\text{TCNQ}]_2^{2-}$  dimers are arranged in chains in the crystal. The chain axis is determined by the symmetry centers  $(0,0,1/2)$  of the dimers and is parallel to the  $[\bar{1}10]$  direction. The neighboring TCNQ molecules in the chain are equidistant with a distance of 8.28 Å between centers of the six membered rings. Bonding the TCNQ molecules into dimers results in an intradimer distance of 1.63 Å between C(38) and C(38'), and an interdimer distance of 3.88 Å between C(35) and C(35') at the terminal ends of the adjacent dimers in the chain. The chains are well separated by  $[\text{Cu}(\text{DMP})_2]^+$  complexes. The chain structure is shown in Figures 6a and 6b.

Electron Paramagnetic Resonance Results- The EPR spectrum at room temperature consists of one, very weak line at the free radical field position ( $g \approx 2$ ) with an orientation dependent linewidth. With increasing temperature a doublet of EPR lines appears, and this doublet gains intensity with increasing temperature. Typical spectra along three orthogonal directions are shown in Figure 7. The doublet spectrum can be identified with the fine structure of an  $S = 1$  excited state of the  $[\text{TCNQ}]_2^{2-}$  dimer. The intensity changes with temperature are fully reversible up to 470 K. At higher temperatures an irreversible decrease in intensity of the triplet fine structure lines is observed as a result of thermal decomposition of the crystal.

A typical high temperature EPR spectrum consists of a central line at  $g = 2.0025$ , and two fine structure lines which

are comparable in amplitude with the central line and symmetrically displaced from the central line. At some crystal orientations in the magnetic field, when the linewidth is relatively large, an additional narrow ( $\Delta B_{pp} = 1.8$  G) line superimposed on the central line may be observed. Finally, as shown in Figure 8, a half-field transition line ( $M_S = \pm 2$ ) may be observed at  $g \approx 4$  in the spectrum of powdered samples.

We will show that the triplet state fine structure lines arise from dipole-dipole coupled radical anions which result from the thermal breaking of the long, exocyclic carbon-carbon sigma bond, and that the central line is probably related to isolated TCNQ<sup>-</sup> radical anions in the chains described above. No spectral features which could be related to copper(II) complexes, or to charge transfer excited states of the DMP ligand<sup>28</sup> were observed.

Angular Dependence of EPR Spectra- The fine structure splitting and the linewidth of the central and fine structure lines are orientation dependent. These angular variations have been recorded at 10° intervals in the three orthogonal planes of the 1,2,3-coordinate system, and the results are presented in Figures 9a, 9b, and 9c.

Triplet State EPR Spectra- Experimental values of the fine structure splitting have been fitted to a general second-rank D-tensor anisotropy equation:<sup>29</sup>

$$D_i(\theta) = \alpha_i + \beta_i \cos 2\theta + \gamma_i \sin 2\theta \quad (1)$$



where  $\theta$  is the azimuthal angle of the magnetic field for the  $i$ -th rotation of the crystal. The anisotropy parameters  $\alpha$ ,  $\beta$ ,  $\gamma$  have been calculated for each rotation by least-squares methods. For a constant  $\theta$  interval, we have the following expressions for the anisotropy parameters:

$$\alpha = n^{-1} \sum_{\theta=0^{\circ}}^M D(\theta)$$

$$\beta = 2n^{-1} \sum_{\theta=0^{\circ}}^M D(\theta) \cos 2\theta \quad (2)$$

$$\gamma = 2n^{-1} \sum_{\theta=0^{\circ}}^M D(\theta) \sin 2\theta$$

where  $n$  and  $M$  are determined by the  $\theta$  interval chosen. These parameters are 36 and  $175^{\circ}$  for  $5^{\circ}$  rotation intervals and 18 and  $170^{\circ}$  for  $10^{\circ}$  intervals. The anisotropy parameters for the three orthogonal rotations have been corrected for zero-angle errors by a modified Waller-Rogers method<sup>30</sup> using programs written for a Tektronix 4052 microcomputer. The results indicated that the experimental error in angle measurements is less than  $\pm 2^{\circ}$ . The

D-tensor components were calculated, and the D-tensor was then diagonalized by standard methods. Principal values and direction cosines are summarized in Table III, and  $D(\theta)$  plots for these data are given by the solid lines in Figures 9a, 9b, and 9c. Using the spin Hamiltonian for the  $S = 1$  case

$$\mathcal{H} = g\mu_B(B_x\hat{S}_x + B_y\hat{S}_y + B_z\hat{S}_z) + D(\hat{S}_z^2 - 2/3) + E(\hat{S}_x^2 - \hat{S}_y^2) \quad (3)$$

we obtained the fine structure parameters  $D/hc = -3D_z/2 = 0.0111 \text{ cm}^{-1}$  and  $E/hc = (D_y - D_x)/2 = 0.0015 \text{ cm}^{-1}$ . The g-factor is isotropic within experimental error and  $g=2.0025(5)$ .

Half-Field Transition- The  $\Delta M_S = \pm 2$  forbidden transition is observed in the spectrum of a powdered sample as a single, symmetrical, Lorentzian-shaped line with  $\Delta B_{pp} = 3.7 \text{ G}$  at  $1620.2 \text{ G}$  ( $g = 4.0430$ ). Because of the very small size of the crystal used for this study, the half-field line could not be observed in the single crystal spectrum. The position of the half-field line in a powder spectrum is given by the Kottis-Lefebvre equation:<sup>31</sup>

$$B_{1/2} = (2g\mu_B B_0)^{-1} [(g\mu_B B_0)^2 - 4(D^2 + 3E^2)/3]^{1/2} \quad (4)$$

Substitution of the measured D and E values (Table III) into Equation (4) results in a prediction of  $B_{1/2} = 1621.9 \text{ G}$  at  $\nu = 9.17 \text{ GHz}$  which is in good agreement with the experimental value.

The intensity ratio of the allowed and forbidden transitions can be evaluated<sup>32</sup> as  $(D/g\mu_B B_0)^2 = 1:100$ . The experimentally estimated value of the intensity ratio was 1:650.

Linewidth of Central and Fine Structure Lines- The central line and the fine structure lines of the triplet state are of Gaussian shape and the peak-to-peak linewidth varies with crystal orientation in the range 3 to 9.8 G and 5 to 12.4 G, respectively. The amplitude (A) of the lines has been measured and relative  $\Delta B_{pp}$  values have been calculated from the integrated intensity relationship  $A \cdot (\Delta B_{pp})^2 = \text{constant}$ . Angular variations of the  $\Delta B_{pp}$  presented in Figure 9 indicate the same angular behavior for the triplet state lines and the central line. This behavior is very similar to that of the D-tensor. Therefore, the linewidth of the triplet state fine structure lines can also be described as a tensor in the crystal. Following the same procedure as in the D-tensor calculation, the principal values and direction cosines of the  $\Delta B_{pp}$ -tensor were determined and are listed in Table III. Plots of  $\Delta B_{pp}(\theta)$  with the parameters given in Table III are given by the solid lines in Figures 9a, 9b, and 9c.

Temperature Dependence of the EPR Spectra- Both the central line and the fine structure lines of the triplet state are thermally activated. At room temperature an impurity signal ( $g = 2.0023$ ) dominates the central line ( $g = 2.0025$ ) in the spectrum. This signal displays Curie-law behavior down to 100 K. At higher temperatures the central line increases in intensity and the

excited triplet state fine structure lines appear. The triplet state fine structure lines gain in intensity more rapidly than the central line, and at 395 K, the intensities of both types of lines are equal. At higher temperatures the triplet state fine structure lines dominate the EPR spectra.

The linewidths of the triplet fine structure lines and of the central line are temperature-independent. Thus,  $\Delta B_{pp}$  is not determined by relaxation processes in the crystal. The integrated intensity  $I \propto A \cdot (\Delta B_{pp})^2$ , which is proportional to the number of unpaired spins is, therefore, simply proportional to the amplitude of the EPR lines. As shown in Figure 10, the temperature dependence of the the EPR spectral intensity is isotropic in single crystal samples. The g-values of the central and fine structure lines are temperature independent. The fine structure splitting parameters are also constant over the temperature range studied, except in the region where thermal decomposition occurs. There the splitting decreases slightly with simultaneous broadening of the lines.

## DISCUSSION

EPR of the  $\sigma$ -Bonded Dimer  $[\text{TCNQ}]_2^{2-}$  - Sigma-bonded TCNQ dimers are rare compared to  $\pi$ -bonded dimers or charge transfer complexes. The  $\sigma$ -bond may be expected to be relatively weak because of the long bond distance, the considerable delocalization of the bonding electrons, and electrostatic

repulsions. Breaking this long, weak sigma bond results in the formation of two TCNQ<sup>-</sup> radical anions constrained in close proximity in the solid state. Dipole-dipole and possibly exchange interactions couple these two radical anions into singlet and triplet states. These expectations are borne out by the observation of thermally-activated triplet state EPR spectra in [Pt(bpy)<sub>2</sub>][TCNQ]<sub>2</sub>,<sup>11</sup> (NEP)<sub>2</sub>[TCNQ]<sub>2</sub>,<sup>12</sup> and now in [Cu(DMP)<sub>2</sub>]<sub>2</sub>[TCNQ]<sub>2</sub>.

The observed excited state EPR spectrum of the [TCNQ]<sub>2</sub><sup>2-</sup> dimer has parameters which may be understood in terms of pairwise dipolar coupling of the unpaired electrons, although an exchange interaction can not be ruled out completely. The values of the dipolar splitting (D-tensor components) reflect a spatial distribution of the correlated spins over the TCNQ molecules. The orientation of the D-tensor principal axes is determined by the symmetry of that distribution, and a knowledge of the unpaired electron density on the constituent atoms of the dimeric pair permits a calculation, in the point-dipole approximation, of the tensor components.

If after bond cleavage, the unpaired spins were fully localized on carbon atoms C(38) and C(38') in the excited state, the D-tensor should be axially symmetrical and the maximum principal value of the dipolar splitting may be calculated to be 2100 G along the C(38)-C(38') directions. That this approximation strongly overestimates the observed splitting values may be understood in terms of delocalization of the spin

density over the TCNQ<sup>-</sup> radical anions.

The spin density  $\rho_i$  distribution may be calculated using semiempirical INDO methods and molecular structural data.<sup>33</sup> Such spin density distributions are known for the TCNQ<sup>-</sup> anion,<sup>34,35</sup> and for the excited state of the  $\sigma$ -bonded dimer in (NEP)<sub>2</sub>[TCNQ]<sub>2</sub>.<sup>12</sup> The pertinent data are collected in Table IV. The molecular structure of the  $\sigma$ -bonded [TCNQ]<sub>2</sub><sup>2-</sup> dimer in [Cu(DMP)<sub>2</sub>]<sub>2</sub>[TCNQ]<sub>2</sub> is similar to that of the dimer in (NEP)<sub>2</sub>[TCNQ]<sub>2</sub>, and we used the  $\rho_i$ -values from Table IV for calculations of D-tensor components for a model in which the two TCNQ<sup>-</sup> radical anions retain the structure exhibited by the bonded dimer. In the point-dipole approximation those components are given by Equation (5):

$$D_{mn} = (1/2)g^2\mu_B^2 \sum_{\substack{i \in A \\ j \in B}} \rho_i \rho_j (r_{ij}^{-2} - 3m_{ij}n_{ij})r_{ij}^{-5} \quad (5)$$

In Equation (5),  $\underline{m}, \underline{n} = x, y, z$  and  $r_{ij} = |\underline{r}_i - \underline{r}_j|$ , and the summation runs over all of the atoms in the pairs of TCNQ<sup>-</sup> radical anions of bond-cleaved dimer.  $D_{mn}$  values have been calculated from the structural data using computer programs which have been described in previous papers.<sup>12,17</sup> The results are presented in Table V.

If one uses the spin densities from the ab initio calculation for a TCNQ<sup>-</sup> anion with idealized D<sub>2h</sub> symmetry<sup>34</sup> ("normal" TCNQ<sup>-</sup> ion) then the calculated fine structure tensor components are overestimated by factors of 2.5 to 4. If,

instead, one chooses INDO<sup>33</sup> spin densities calculated<sup>12</sup> for a distorted TCNQ<sup>-</sup>  $S = 1/2$  ion (with atom positions in the (NEP)<sub>2</sub>[TCNQ]<sub>2</sub> structure<sup>12</sup>) then the theoretical  $D_x$ ,  $D_y$ ,  $D_z$  values ("distorted" TCNQ<sup>-</sup> ions in Table V) exceed the experimental values by even larger factors. This arises because the distortion about atom C(38) concentrates the spin density at C(38) (see Table IV), the atom involved (in the ground state) in the exocyclic sigma bond. This increased disagreement between theory and experiment has been noticed before<sup>12</sup> and may be understood in the following way. The expected Coulomb repulsion between the two TCNQ<sup>-</sup> radicals in the  $S = 1$  state is not relieved by an exchange interaction between the [TCNQ]<sub>2</sub><sup>2-</sup>  $S = 1$  dianion and nearest-neighbor  $S = 0$  [TCNQ]<sub>2</sub><sup>2-</sup> dianions, because of negligible overlap between [TCNQ]<sub>2</sub><sup>2-</sup> in [Cu(DMP)<sub>2</sub>]<sub>2</sub>[TCNQ]<sub>2</sub> along the [110] chain direction.

Thus, as before,<sup>12</sup> if one uses a triplet state spin distribution obtained by an inversion of the distorted TCNQ<sup>-</sup> radical anion, that is, by interchanging the spin density of C(38) with that of C(35), C(30) with C(37), etc. ("distorted and inverted" TCNQ<sup>-</sup> ions in Table V) then much better agreement is obtained between the theoretical and experimental  $D_x$ ,  $D_y$ , and  $D_z$  values. This agreement is nearly as good as that obtained between theory and experiment in pi-bonded dimers.<sup>14,16,17,35,36</sup>

Since there is a limited amount of "free space" around the [TCNQ]<sub>2</sub><sup>2-</sup> dianion in the crystal lattice, one expects some geometrical rearrangement as the dianion is excited from the  $S =$

0 to the  $S = 1$  state. One may speculate, in particular, that the  $C(38)-C(38')$  distance may increase. As a result it is difficult to predict theoretically the exact equilibrium geometry of the  $S = 1$  state. Any fitting of "better" spin densities to experiment in the spirit of Ref. 36 may be unadvisable since the TCNQ<sup>-</sup> ions are, in part, much closer than normal van der Waals distances.

A comparison between the experimental and theoretical orientations of the  $D_x$ ,  $D_y$ , and  $D_z$  axes given in Tables V and VI indicates some discrepancies in these values for all three theoretical models. For the "distorted and inverted" spin density model, the largest difference in direction angles between theory and experiment is less than  $12^\circ$ . Thus, the symmetry of the spin density distribution is fairly well given by the model and reflects the distortion in the excited state as observed in other crystals.<sup>12,16,17</sup> Experimentally the z-axis of the D tensor deviates  $18.5^\circ$  from the  $C(38)-C(38')$  direction, while the theoretical "distorted and inverted" model predicts a deviation of  $19.9^\circ$ . The data in Table VI also indicate that there is no relationship between the D-tensor axes and TCNQ-chain axis  $[\bar{1}10]$  in the crystal.



Triplet Excited State Dynamics- The dynamical behavior of the spins in the triplet state is expected to affect the linewidth and temperature dependence of the EPR spectrum. There are three features of the EPR lines in the spectra of  $[\text{Cu}(\text{DMP})_2]_2[\text{TCNQ}]_2$  which have a bearing on this point: these are the relatively large  $\Delta B_{pp}$ , the lack of hyperfine splitting of the central and fine structure lines, and the similarity of the angular variation of  $\Delta B_{pp}$  with that of the D-tensor.

The broad EPR lines indicate that the excited state is localized on the  $[\text{TCNQ}]^-$  radical anions. Therefore, the data may be described in terms of self-trapping Frenkel excitons. The absence of hyperfine splitting is generally considered to result from a dynamical averaging effect from translation or diffusion of the triplet excitons through the crystal. Theoretical considerations of the linewidth in TCNQ crystals take into account, moreover, an interchain hopping or diffusion of excitons, and the effect of exciton-exciton interactions.<sup>8,37</sup> Interchain hopping is probably unimportant in determining the linewidth in  $[\text{Cu}(\text{DMP})_2]_2[\text{TCNQ}]_2$  since the TCNQ chains are well separated by the large  $[\text{Cu}(\text{DMP})_2]^+$  cations. If exciton-exciton interactions were important, then  $\Delta B_{pp}$  would be proportional to the density of triplet excitons and show an increase with temperature. As noted above,  $\Delta B_{pp}$  is independent of temperature in  $[\text{Cu}(\text{DMP})_2]_2[\text{TCNQ}]_2$ .

It appears that the linewidth is due to overlapping and broadening of hyperfine lines. Data for TCNQ<sup>-</sup> radical anions<sup>38</sup> indicates that hyperfine splitting is about 0.52 G for <sup>14</sup>N and 0.72 G for <sup>1</sup>H nuclei. Overlapped hyperfine splitting from four protons and four nitrogen atoms of [TCNQ]<sup>-</sup> should result in a broad EPR line with  $\Delta B_{pp}$  of 5 to 8 G, in good agreement with the  $\Delta B_{pp}$  values for the triplet state lines in [Cu(DMP)<sub>2</sub>]<sub>2</sub>[TCNQ]<sub>2</sub> (see Figure 9). Moreover, the lines are Gaussian in shape, as is expected in the case of unresolved hyperfine structure.

The similarity in the angular variation in D and  $\Delta B_{pp}$  could suggest that the linewidth may be due to a random distribution of D-values in the crystal. This possibility, usual in transition metal ion EPR spectra, is considered to be a broadening effect arising from randomly distributed strains in crystals.<sup>39,40</sup> This is probably not the case in our crystals since the angular variation of  $\Delta B_{pp}$  for the triplet lines is identical with that for the central ( $S = 1/2$ ) line, and the central line can not be related to a distribution of D-values. Furthermore, as shown in Table III, the principal directions of the D-tensor and the  $\Delta B_{pp}$ -tensor do not coincide exactly. The broadest EPR line appears along a direction which deviates from the C(38)-C(38') direction toward the centers of the pairs of dipole coupled [TCNQ]<sup>-</sup> radical anions. This deviation is toward the direction expected for maximum hyperfine splitting from the hydrogen atoms of the six membered ring, an observation that supports the conclusion that  $\Delta B_{pp}$  arises from unresolved

hyperfine splitting.

Temperature Dependence of Intensities- The integrated intensity  $I$  of the triplet state fine structure lines is strongly temperature dependent. The value of the intensity is related to the microwave power ( $A_0 = \chi_0 \omega_0^2 B_1^2 T_2 / 4$ ) absorbed by a sample under resonance conditions. The microwave frequency  $\omega_0$  and microwave field intensity  $B_1$  were held constant during intensity measurements. Furthermore, the temperature independent  $\Delta B_{pp}$ -values indicate that the relaxation time  $T_2$  does not affect the linewidth. Thus, the EPR line intensity is simply proportional to the static magnetic susceptibility  $\chi_0$  of the sample.

The energy levels which are populated and determine the magnetic properties of  $[\text{Cu}(\text{DMP})_2]_2[\text{TCNQ}]_2$  are sketched in Figure 11 for two cases, those being split in the excited state by isotropic exchange only (Fig. 11a), or by dipolar interaction only (Fig. 11b). It is possible that the excited  $S=1$  state arises from weak antiferromagnetic exchange of the unpaired electrons from the broken  $\sigma$ -bond. In this case the magnetic susceptibility derived from the Van Vleck equation gives the following expression for the relative intensity of the EPR signal:

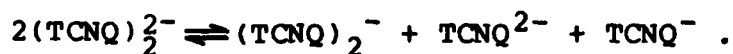
$$I \propto (1/T) [\exp(-E_a/k_B T)] [1 + 3 \exp(-E_a/k_B T) + \exp(-E_a/k_B T + 2J/k_B T)]^{-1} \quad (6)$$

A fit of Equation (6) to the experimental intensity data yields two results: (i)  $E_a = 0.55$  eV (51.5 kJ/mol) and  $2J = 0$ ; (ii)  $E_a = 0$  and  $2J = -0.55$  eV. The latter fitting results can be dismissed<sup>56</sup> because of the experimental zero-field splitting tensor is traceless within the experimental error in  $[\text{Cu}(\text{DMP})_2]_2[\text{TCNQ}]_2$ . Thus, the exchange interaction is very small in the excited state of the  $\text{TCNQ}_2^{2-}$  dimer and can be estimated to be  $J < 10^{-4} \text{ cm}^{-1}$ . The unpaired electrons are, thus, essentially coupled by dipolar interaction only, as presented in Fig. 11b, with  $D/hc = 0.0111 \text{ cm}^{-1}$ . Since the zero-field splitting is much smaller than  $E_a$ , this splitting does not influence the magnetic susceptibility of the system. Thus, the system is not a triplet state of the  $\text{TCNQ}_2^{2-}$  dimer, but a dipole-dipole coupled biradical with activation energy  $E_a = 0.55$  eV. A plot of Equation (6) with  $E_a = 0.55$  eV and  $2J = 0$  is given as the solid line in Figure 10.

The absolute number of spins in the triplet state has been determined as  $0.12(5) \times 10^{18}$  spins/g at 327 K. The number of broken C(38)-C(38')  $\sigma$ -bonds producing biradical states as a result of thermal excitations is 0.028% at 327 K and 1.7% at 409 K (See Table VII). If one accepts  $E_a = 0.55$  eV as the energy required to break the C(38)-C(38') sigma bond (with concomitant geometrical rearrangements in the  $S = 1$  state) then one should question why the corresponding activation energy is only 0.27 eV in  $(\text{NEP})_2[\text{TCNQ}]_2$ . Either the molecular rearrangement presents a larger Franck-Condon barrier in  $[\text{Cu}(\text{DMP})_2]_2[\text{TCNQ}]_2$ , or else the

existence of the "chain" of TCNQ dimers in  $[\text{Cu}(\text{DMP})_2]_2[\text{TCNQ}]_2$ , albeit with small overlap, provides extra stabilization of the ground state.

Central ( $S = 1/2$ ) EPR Signal- EPR signals at  $g \approx g_e$  are generally observed in TCNQ crystals. In most cases these lines are explained as signals from paramagnetic organic impurities or crystal imperfections. In our crystal, however, at room temperature there are two overlapping lines at  $g \approx g_e$ . At room temperature and below there is a broad thermally activated line which nearly obscures a narrow line that gains in intensity as the temperature is decreased. The narrow line with Curie-Weiss behavior is attributed to an impurity or defect signal. The broader, thermally activated line ( $g = 2.0025$ ) exhibits the same angular dependence of linewidth as the triplet fine structure lines and we speculate that it arises from isolated  $\text{TCNQ}^-$  radical anions or  $(\text{TCNQ})_2^-$  ions which result from disproportionation according to the following



The behavior of the broader central line is similar to that found in morpholinium TCNQ salts.<sup>7,10</sup> The signal is thermally activated with an EPR line intensity  $I \propto (1/T)\exp(-E_a/k_B T)$ . The experimental data gives  $E_a = 0.24$  eV (22.6 kJ/mol) for temperatures greater than 350 K. Below this temperature the impurity signal is comparable in amplitude with the central line, and the experimental points deviate from the  $I(T)$  dependence observed at higher temperatures. The number of spins

responsible for the central signal is equal to  $3.9 \times 10^{18}$  spins/g at 394 K, where the intensities of the triplet state fine structure signals and the central signal are identical.

The very narrow EPR signal ( $g = 2.0025$ ) which is observed only at higher temperatures and is superimposed on the central line can be related to a small number of highly mobile  $\text{TCNQ}^-$  lattice misfits. These mobile misfits give rise to the motionally narrowed EPR line as a result of a translational motion along the TCNQ chain.

#### CONCLUSIONS

In  $[\text{Cu}(\text{DMP})_2]_2[\text{TCNQ}]_2$ ,  $\text{TCNQ}^-$  radical anions are arranged in chains with  $\sigma$ -bonds between pairs of  $\text{TCNQ}^-$  ions. The sigma bond is weak and may be thermally cleaved with an activation energy of 0.55 eV. Thermally activated EPR signals are related to a triplet excited state arising from dipolar coupling of pairs of  $\text{TCNQ}^-$  radical anions, and doublet state ( $E_a = 0.24$  eV) associated with isolated  $\text{TCNQ}^-$  radical anions.

The activation energy for the biradical state arising from bond cleavage is the largest yet observed in sigma bonded  $\text{TCNQ}^-$  dimers (see Table VIII). The triplet excitations are largely localized, presumably as a result of the structure of the TCNQ chain which is not optimized for the formation of highly mobile excitons. There was no indication of a phase transition to a paramagnetic phase similar to the phase transition observed in

stabilization of the ground state of the TCNQ trimer by hydrogen bonding with the morpholinium molecules in the crystal.

The insensitivity of the D values for the sigma-bonded dimers to the activation energy implies that the primary interaction leading to the zero-field splitting is not dependent on the population of the triplet state. Thus, D values are intrinsic properties of isolated pairs of coupled radicals arising from the cleavage of the sigma bond. Furthermore, the constancy of the D values indicates that the molecular and electronic structure in the triplet state is very similar for all three sigma-bonded  $[\text{TCNQ}]_2^{2-}$  dimers.

#### ACKNOWLEDGEMENTS

This research was supported in part by the Office of Naval Research and the National Science Foundation through Grants CHE 80 09685 (Univ. of North Carolina) and DMR 80 15658 (Univ. of Mississippi). We are also grateful to the National Science Foundation for partial funding of the purchase of the EPR spectrometer through grant no. CHE 80 06078, and we wish to thank Professor H. J. Keller for insightful discussions.

#### SUPPLEMENTARY MATERIAL AVAILABLE:

Anisotropic thermal parameters (3 pages). Ordering information is given on any current masthead page.

## REFERENCES

- (1) University of North Carolina. (a) Permanent Address:  
Institute of Molecular Physics, Polish Academy of Sciences,  
60-179 Poznan , Poland. (b) Present Address: Eastman Kodak  
Co., Rochester, N. Y.
- (2) University of Mississippi.
- (3) Nordio, P. L.; Soos, Z. G.; McConnell, H. M. Ann. Rev. Phys. Chem. 1966, 17, 237-260.
- (4) Hatfield, W. E., Editor, "Molecular Metals", NATO Conference  
Series VI, Vol 1, Plenum Press:New York, 1979.
- (5) Gordy, W. "Theory and Applications of Electron Spin  
Resonance", John Wiley, New York, 1980.
- (6) Yagubskii, E. B.; Khidekel, M. L. Russian Chem. Revs. 1972,  
41, 1011-1026.
- (7) Soos, Z. G. Ann. Rev. Phys. Chem. 1974, 25, 121-153.
- (8) Hibma, T.; Kommandeur, J. Phys. Rev. Sect. B 1975, B12,  
2608-2618.
- (9) Takagi, S.; Kawabe, K. Solid State Commun. 1976, 18, 1467-  
1470.
- (10) Kepler, R. G. J. Chem. Phys. 1963, 39, 3528-3532.
- (11) Dong, V.; Endres, H.; Keller, H. J.; Moroni, W.; Nothe, D.  
Acta Cryst. Sect. B 1977, B33, 2428-2431.
- (12) Harms, R. H.; Keller, H. J.; Nothe, D.; Werner, M.  
Gundel, D.; Sixl, H.; Soos, Z.; Metzger, R. M. Mol. Cryst. Liq. Cryst. 1981, 65, 179-196.



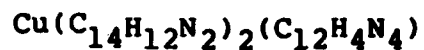
- (13) Hibma, T.; Dupuis, P.; Kommandeur, J. Chem. Phys. Letters 1972, 15, 17-20.
- (14) Marechal, M. A.; McConnell, H. M. J. Chem. Phys. 1965, 43, 497-498.
- (15) Bailey, J. C.; Chesnut, D. B. J. Chem. Phys. 1969, 51, 5118-5128.
- (16) Harms, R. H.; Keller, H. J.; Nothe, D.; Wehe, D.; Heimer, N.; Metzger, R. M.; Gundel, D.; Sixl, H. Mol. Cryst. Liq. Cryst. 1982, 85, 249.
- (17) Metzger, R. M.; Heimer, N. E.; Gundel, D.; Sixl, H.; Harms, R. H.; Keller, H. J.; Nothe, D.; Wehe, D. J. Chem. Phys. in press.
- (18) Chesnut, D. B.; Arthur, P. J. Chem. Phys. 1962, 36, 2969-2975.
- (19) Chesnut, D. B.; Phillips, W. D. J. Chem. Phys. 1961, 35, 1002-1012.
- (20) Thomas, D. D.; Merkl, A. W.; Hildebrandt, A. F.; McConnell, H. M. J. Chem. Phys. 1964, 40, 2588-2594.
- (21) Flandrois, S.; Amiell, J.; Carmona, F.; Delhaes, P. Solid State Commun. 1975, 17, 287-290.
- (22) Endres, H.; Keller, H. J.; Moroni, W.; Nothe, D. Z. Naturf. 1976, 31b, 1322-1325.
- (23) Soos, Z. G.; Klein, D. J. J. Chem. Phys. 1971, 55, 3284-3290.
- (24) Vegter, J. G.; Kommandeur, J. Mol. Cryst. Liq. Cryst. 1975, 30, 11-49.

- (25) Hall, J. R.; Marchant, N. K.; Plowman, R. A.  
Austr. J. Chem. 1963, 16, 34-41.
- (26) Johnson, C. K. Report No. ORNL-3794, Oak Ridge National Laboratory, Oak Ridge, TN.
- (27) Morosin, B.; Plastas, H. J.; Coleman, L. B.; Steward, J. M.  
Acta Cryst. Sect. B 1978, B34, 540-543.
- (28) Ahn, B. T.; McMillan, D. R. Inorg. Chem. 1981, 20, 1427-1432.
- (29) Weil, J. A.; Buch, T.; Clapp, J. E. Adv. Magn. Res. 1973, 6, 183-257.
- (30) Waller, W. G.; Rogers, M. T. J. Magn. Res. 1975, 18, 39-56.
- (31) Kottis, P.; Lefévre, R. J. Chem. Phys. 1963, 39, 393-403.
- (32) Smith, T. D.; Pilbrow, J. R. Coord. Chem. Revs. 1974, 13, 173-278.
- (33) Pople, J. A.; Beveridge, D. L. "Approximate Molecular Orbital Theory", McGraw-Hill: New York, 1970.
- (34) Jonkman, H. T.; van der Welle, G.; Nieuport, W. C. Chem. Phys. Letters 1974, 25, 62-65.
- (35) Silverstein, A. J.; Soos, Z. G. Chem. Phys. Letters 1976, 39, 525-530.
- (36) Flandrois, S.; Boissonade, J. Chem. Phys. Letters 1978, 58, 596-600.
- (37) Hibma, T.; Sawatzky, G. A.; Kommandeur, J. Phys. Rev. Sect. B 1977, B15, 3959-3966.

- (38) Brown, I. M.; Jones, M. T. J. Chem. Phys. 1969, 51, 4687-4694.
- (39) Feher, E. R. Phys. Rev. 1964, 136A, 145-156.
- (40) Hagen, W. R. J. Magn. Res. 1981, 44, 447-469.
- (41) Hoekstra, A.; Spoelder, T.; Ves, A. Acta Cryst. 1972, B28, 14-25.
- (42) Sakai, N.; Shirotani, I.; Minomura, S. Bull. Chem. Soc. Japan 1972, 45, 3321-3328.
- (43) Van Bodegom, B.; de Boer, J. L.; Ves, A. Acta Cryst. 1977, B33, 602-604.
- (44) Sundaresan, T.; Wallwork, S. C. Acta Cryst. 1972, B28, 3507-3511.
- (45) Chasseau, D.; Gaultier, J.; Hauw, C. Compt. Rend. Acad. Sci. (Paris) 1972, 274C, 1434-1437.
- (46) Chasseau, D.; Gaultier, J.; Hauw, C.; Schwoerer, M. Comp. Rend. Acad. Sci. (Paris) 1972, 275C, 1491-1493.
- (47) Chonkrown, M. L. Ph. D. Thesis, Univ. Bordeaux I, 1977.
- (48) Fritchie, C. J.; Arthur, P. Acta Cryst. 1966, 21, 139-145.
- (49) Sundaresan, T.; Wallwork, S. C. Acta Cryst. 1972, B28, 491-497.
- (50) Konno, M.; Saito, Y. Acta Cryst. 1973, B29, 2815-2824.
- (51) McPhail, A. T.; Semenink, G. M.; Chesnut, D. B. J. Chem. Soc. Part A 1971, 2174-2180.
- (52) Kobayashi, H.; Ohashi, Y.; Marumo, F.; Saito, Y. Acta Cryst. 1970, B26, 459-467.

- (53) Potworowski, J. A. Ph. D. Thesis, Univ. of Toronto, 1973.
- (54) Chasseau, D. These, Univ. de Bordeaux I, 1979.
- (55) Gundel, D.; Sixl, H.; Metzger, R. M.; Heimer, N. E.;  
Harms, R. H.; Keller H. J.; Nothe, D.; Wehe, D.  
in preparation.
- (56) Coffman, R. E.; Buettner, G. R. J. Phys. Chem.  
1979, 83, 2392-2400.

Table I. Crystal Data and Data Collection Summary for



FW	684.3
Space Group	$\text{P}\bar{1}$
Cell Dimensions	
a, Å	12.784(6)
b, Å	13.400(6)
c, Å	12.136(4)
$\alpha$ , deg	113.51(3)
$\beta$ , deg	112.58(3)
$\gamma$ , deg	62.80(3)
U, Å <sup>3</sup>	1643.0
Z	2
Cryst dims, mm	0.38 x 0.25 x 0.10
Radiation	MoK $\alpha$ ( $\lambda = 0.71069$ Å)
$\mu$ , cm <sup>-1</sup>	7.1
2 $\theta_{\text{max}}$ , deg	27.5
Scan type	$\omega/2\theta$
Unique data measd	4500
Unique data used	1957
$[F_o^2 > 3\sigma(F_o^2)]$	
R	0.060
$R_w$	0.070

Table II. Positional Parameters for  $[\text{Cu}(\text{DMP})_2]_2[\text{TCNQ}]_2$ 

Atom	x	y	z
Cu	0.2024(1)	0.1657(1)	0.2266(1)
N1	0.2912(6)	-0.0048(6)	0.1474(6)
N2	0.2259(7)	0.1894(7)	0.0794(7)
N3	0.0359(6)	0.2423(7)	0.2643(7)
N4	0.2601(6)	0.2436(6)	0.4153(6)
N5	0.2681(9)	0.5235(8)	-0.0251(8)
N6	0.5352(10)	0.4203(9)	0.3087(10)
N7	-0.2131(7)	0.9363(7)	0.4288(7)
N8	0.0851(8)	0.9474(7)	0.7411(8)
C1	0.3236(9)	-0.0989(8)	0.1843(10)
C2	0.3913(10)	-0.2085(9)	0.1222(10)
C3	0.4242(10)	-0.2230(9)	0.0162(10)
C4	0.3898(8)	-0.1237(8)	-0.0218(9)
C5	0.3237(8)	-0.0181(9)	0.0450(9)
C6	0.2884(8)	0.0835(8)	0.0110(8)
C7	0.3184(8)	0.0764(8)	-0.0918(8)
C8	0.2854(9)	0.1790(9)	-0.1207(9)
C9	0.2221(10)	0.2829(9)	-0.0505(9)
C10	0.1896(9)	0.2903(8)	0.0540(10)
C11	0.4207(10)	-0.1318(10)	-0.1245(10)

Table II. Continued

Atom	x	y	z
C12	0.3861(9)	-0.0355(10)	-0.1593(9)
C13	0.2809(10)	-0.0820(9)	0.2917(9)
C14	0.1176(11)	0.4026(9)	0.1348(10)
C15	-0.0713(8)	0.2463(8)	0.1953(9)
C16	-0.1781(8)	0.3135(9)	0.2375(9)
C17	-0.1635(9)	0.3623(9)	0.3676(10)
C18	-0.0512(8)	0.3583(8)	0.4451(9)
C19	0.0507(8)	0.2977(8)	0.3954(8)
C20	0.1656(8)	0.3016(8)	0.4673(8)
C21	0.1801(8)	0.3552(8)	0.5929(8)
C22	0.2947(10)	0.3575(9)	0.6575(9)
C23	0.3882(10)	0.3045(10)	0.6058(10)
C24	0.3707(8)	0.2439(9)	0.4763(9)
C25	-0.0299(9)	0.4106(9)	0.5754(9)
C26	0.0792(9)	0.4105(9)	0.6443(10)
C27	0.4716(9)	0.1854(11)	0.4095(11)
C28	-0.0766(10)	0.1808(10)	0.0581(9)
C29	0.2478(8)	0.6483(8)	0.2809(9)
C30	0.1272(9)	0.7044(8)	0.2334(9)
C31	0.0494(9)	0.7953(8)	0.3003(9)

Table II. Continued

Atom	x	y	z
C32	0.0915(8)	0.8302(8)	0.4306(8)
C33	0.2100(9)	0.7735(8)	0.4798(9)
C34	0.2869(8)	0.6813(8)	0.4151(9)
C35	0.3315(9)	0.5560(9)	0.2120(9)
C36	0.2954(10)	0.5373(9)	0.0807(9)
C37	0.4447(10)	0.4838(10)	0.2644(10)
C38	0.0064(8)	0.9376(7)	0.5031(8)
C39	-0.1160(8)	0.9370(8)	0.4606(8)
C40	0.0508(8)	0.9401(8)	0.6398(8)
H2	0.4150	-0.2778	0.1482
H3	0.4737	-0.3015	-0.0271
H8	0.3080	0.1804	-0.1885
H9	0.1923	0.3585	-0.0724
H11	0.4678	-0.2082	-0.1746
H12	0.4085	-0.0395	-0.2302
H16	-0.2593	0.3230	0.1794
H17	-0.2350	0.3989	0.4038
H22	0.3081	0.4001	0.7469
H23	0.4714	0.3021	0.6578
H25	-0.0987	0.4502	0.151
H26	0.0911	0.4487	0.7348



Table II. Continued

-----			
Atom	x	y	z
-----			
H30	0.0929	0.6747	0.1439
H31	-0.0339	0.8357	0.2581
H33	0.2418	0.8006	0.5705
H34	0.3665	0.6367	0.4562



Table IV. Spin Densities in TCNQ<sup>-</sup> Anion and [TCNQ]<sub>2</sub><sup>2-</sup> Dianion

Atom	$\rho_i$ Values	
	TCNQ <sup>-</sup>	[TCNQ] <sub>2</sub> <sup>2-</sup>
	normal	distorted
	(Ref. 12, 34)	(Ref. 12)
C29	0.109	0.0715
C30	0.059	0.0331
C31	0.059	0.0512
C32	0.109	0.0618
C33	0.059	0.0531
C34	0.059	0.0351
C35	0.191	0.1226
C36	0.002	0.0130
C37	0.002	0.0015
C38	0.191	0.3491
C39	0.002	0.0085
C40	0.002	0.0076
N5	0.039	0.0356
N6	0.039	0.0376
N7	0.039	0.0620
N8	0.039	0.0640

Table V. Experimental and Theoretical Values (for Spin Density Distributions from Table IV) of D-Tensor Principal Values and Principal Vector Angles in (1,2,3) Reference System

D/hc Values			direction angles, deg		
	$\times 10^4 \text{ cm}^{-1}$		$1 \equiv [\bar{2}\bar{1}0]$	2	$3 \equiv [00\bar{1}]$
<hr/>					
Experimental	$D_x$	$\pm 52$	146.3	73.2	118.3
	$D_y$	$\pm 22$	122.2	100.3	34.2
	$D_z$	$\mp 74$	81.1	19.9	72.3
<hr/>					
Theoretical					
two "normal"					
TCNQ <sup>-</sup> ions	$D_x$	119.8	148.6	95.6	120.8
	$D_y$	84.8	117.3	109.1	34.3
	$D_z$	-204.6	104.4	20.0	76.5
two "distorted"					
TCNQ <sup>-</sup> ions	$D_x$	292.4	148.9	96.3	120.3
	$D_y$	257.1	113.6	118.6	38.5
	$D_z$	-549.5	109.1	29.4	68.5
two "distorted and inverted"					
TCNQ <sup>-</sup> ions	$D_x$	56.3	148.3	95.1	121.1
	$D_y$	35.1	118.7	105.3	33.2
	$D_z$	-91.3	102.2	16.2	79.6
<hr/>					

Table VI. Angles Between Crystal Directions and the Principal Axes  
of the Experimental Tensors and of the Theoretical Fine  
Structure Tensor using the "Distorted and Inverted" Spin  
Density Distribution

Axis	Dimer Bond	Molecular Axis	Chain Axis	Crystallogr. Axes		
	C(38)-C(38')	C(38)-C(35)	[110]	a	b	c
<hr/>						
<u>Experimental</u>						
X(D)	70.1	105.0	96.4	57.0	66.0	61.7
Y(D)	67.4	43.1	111.3	34.2	65.3	145.8
Z(D)	31.9	129.2	22.3	97.9	35.7	107.7
Z( $\Delta B_{pp}$ )	33.7	123.9	22.0	97.1	37.5	113.3
<u>Theoretical</u>						
X(D,inv)	89.3	88.5	117.5	53.7	84.6	58.9
Y(D,inv)	72.7	37.9	114.7	37.6	70.7	146.8
Z(D,inv)	17.3	127.9	38.5	81.5	20.1	100.4

Table VII. Number of Spins and Broken Dimer Bonds at Different  
Temperatures

Temp K	Triplet State				Central Line		
	spin/g $\times 10^{18}$	spin/molecule $\times 10^{-3}$	broken bonds ratio	%	spin/g $\times 10^{18}$	spin/mol $\times 10^{-3}$	ratio
327	0.12	0.14	1/3570	0.028	1.0	1.2	1/833
394	3.9	4.4	1/114	0.9	3.9	4.4	1/227
409	7.5	8.5	1/59	1.7	5.3	6.0	1/167

Table VIII. Zero-Field Splitting Parameters and Activation Energies  
for  $\sigma$ - and  $\pi$ -Bonded Dimers in TCNQ Compounds

No.	Compound	D/hc 10 <sup>4</sup> cm <sup>-1</sup>	E/hc 10 <sup>4</sup> cm <sup>-1</sup>	E <sub>a</sub> eV	EPR Ref	X-Ray Str Ref
<u>Sigma-bonded dimers:</u>						
1.	[Pt(bpy) <sub>2</sub> ][TCNQ] <sub>2</sub>	100	14	0.25	11	11
2.	(NEP) <sub>2</sub> [TCNQ] <sub>2</sub>	104	14	0.27	12	27
3.	[Cu(DMP) <sub>2</sub> ] <sub>2</sub> [TCNQ] <sub>2</sub>	111	15	0.55	this work	
<u>Pi-bonded dimers:</u>						
4.	Li <sub>2</sub> [TCNQ] <sub>2</sub>	154	23	0.23	13	
5.	Rb <sub>2</sub> [TCNQ] <sub>2</sub>	133	16	0.29	8,13,37	41-43
6.	(MPM) <sub>2</sub> [TCNQ] <sub>2</sub>	149	18	0.36	14,15	44
7.	(DMB) <sub>2</sub> [TCNQ] <sub>2</sub>	133	23	0.20	13	45
8.	(TMB) <sub>2</sub> [TCNQ] <sub>2</sub>	144	22	0.17	8,13,37	46
9.	(DMCHA) <sub>2</sub> [TCNQ] <sub>2</sub>	141	16	0.31	13	47
10.	(NBP) <sub>2</sub> [TCNQ] <sub>2</sub>	124	20	0.14	16	16
11.	(NBP) <sub>2</sub> [TCNQF <sub>4</sub> ] <sub>2</sub>	120	21	0.15	17	55
<u>Pi-Bonded Trimeric Dianions</u>						
12.	Rb <sub>2</sub> [TCNQ] <sub>3</sub>	94	11		13	
13.	Cs <sub>2</sub> [TCNQ] <sub>3</sub>	94	15	0.16	13,18	48
14.	(MPM) <sub>2</sub> [TCNQ] <sub>3</sub>	94	15	0.31	15	49

Pi-Bonded Tetrameric Dianions

15. $(\phi_3\text{PCH}_3)_2[\text{TCNQ}]_4$	63	10	0.065	15,19,20	50,51
16. $(\phi_3\text{AsCH}_3)_2[\text{TCNQ}]_4$	63	10	0.065	19	51
17. $(\text{Et}_3\text{NH})_2[\text{TCNQ}]_4$	41	5	0.036	21	52-54

---

Abbreviations: bpy, 2,2'-bipyridine; NEP, N-ethylphenazinium; DMP, 2,9-dimethyl-1,10-phenanthroline; MPM, morpholinium; DMB, 1,3-dimethylbenzimidazolium; TMB, 1,3,5-trimethylbenzimidazolium; DMCHA, diethylmethylbenzimidazolium; NPB, N-butylphenazinium; TCNQF<sub>4</sub>, 2,3,5,6-tetra-fluoroTCNQ;  $\phi_3\text{PCH}_3$ , triphenylmethylphosphonium; Et<sub>3</sub>NH, triethylammonium



## FIGURE CAPTIONS

- Figure 1. Habit of  $[\text{Cu}(\text{DMP})_2]_2[\text{TCNQ}]_2$  crystal with the orthogonal (1,2,3) coordinate system used in EPR measurements. Direction cosines of the (a,b,c) crystallographic axes in the (1,2,3) coordinate system are (0.9159, -0.1172, -0.3840), (0.4352, 0.8072, -0.3989), and (0,0,1), respectively.
- Figure 2. An ORTEP view of the TCNQ dimer showing the mean bond distances and angles. There is a crystallographic center of inversion in the middle of the C(38)-C(38') bond.
- Figure 3. A view of the  $[\text{Cu}(\text{DMP})_2]^+$  cation with the atom numbering system.
- Figure 4. Mean bond distances and angles in the DMP moiety assuming  $C_{2v}$  symmetry.
- Figure 5. A stereoview of the contents of the unit cell looking down the a-axis with the origin in the center, the b-axis going to the right, and the c-axis up.
- Figure 6. Projection of the  $[\text{Cu}(\text{DMP})_2]_2[\text{TCNQ}]_2$  crystal structure along a) the c-axis (axis 3 of the EPR coordinate system), and b) the 1-axis of the EPR coordinate system. The unit

cell edges and directions of the EPR D-tensor principal axes  $x, y, z$  are indicated. The cation  $[\text{Cu}(\text{DMP})_2]^+$  is marked only by the position of the Cu(I) ion.

Figure 7. EPR spectrum of a powdered sample of  $[\text{Cu}(\text{DMP})_2]_2[\text{TCNQ}]_2$  at 393 K ( $\nu = 9.17$  GHz).

Figure 8. EPR spectrum of a single crystal of  $[\text{Cu}(\text{DMP})_2]_2[\text{TCNQ}]_2$  along the principal directions of the D-tensor at 328 K. The separations between the outer lines are:

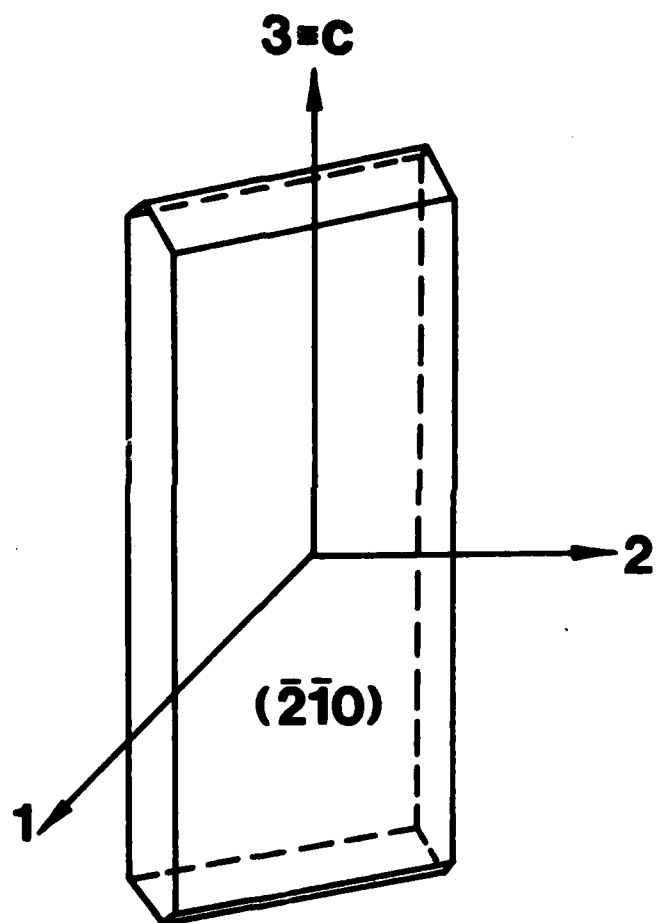
$$\begin{aligned} |D - 3E| &= 3D_{xx} \text{ for } H \parallel x, & |D + 3E| &= 3D_{yy} \text{ for } H \parallel y, \\ 2|D| &= 3D_{zz} \text{ for } H \parallel z. \end{aligned}$$

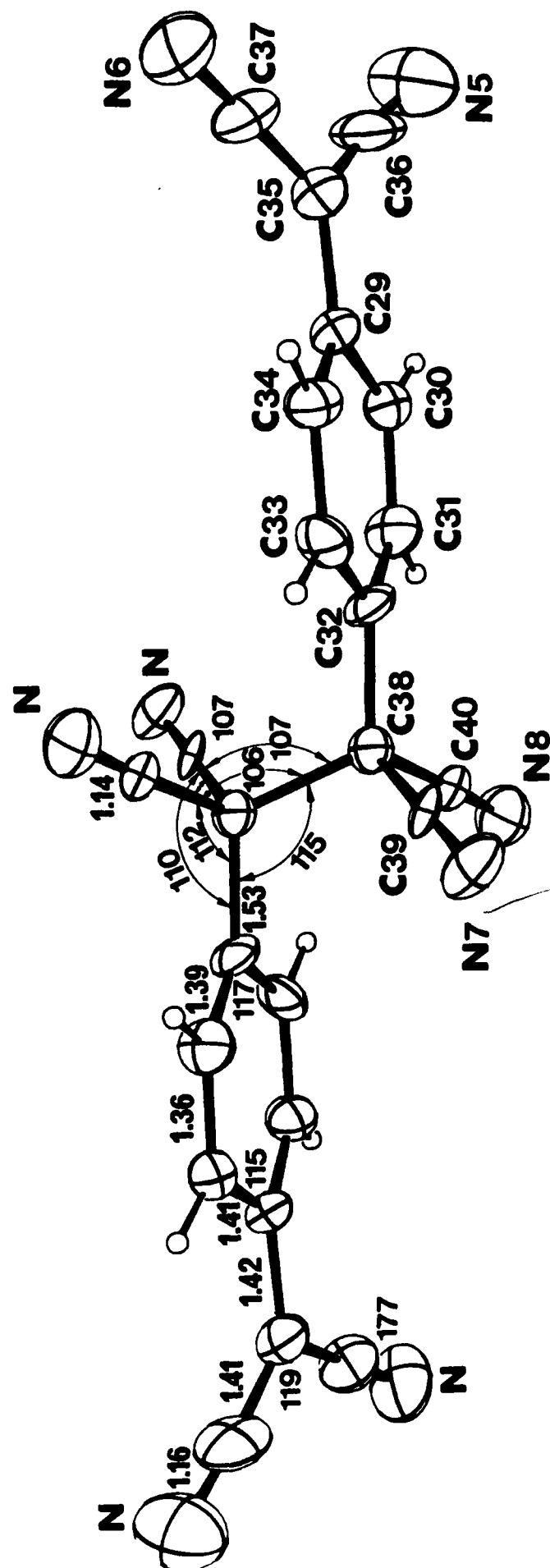
Figure 9. Angular variations of the triplet state fine structure and peak-to-peak linewidths (filled circles) and central EPR line (open circles) in a) 23-plane, b) 31-plane, and c) 12-plane at 328 K. Solid lines are theoretical plots with the parameters given in Table III.

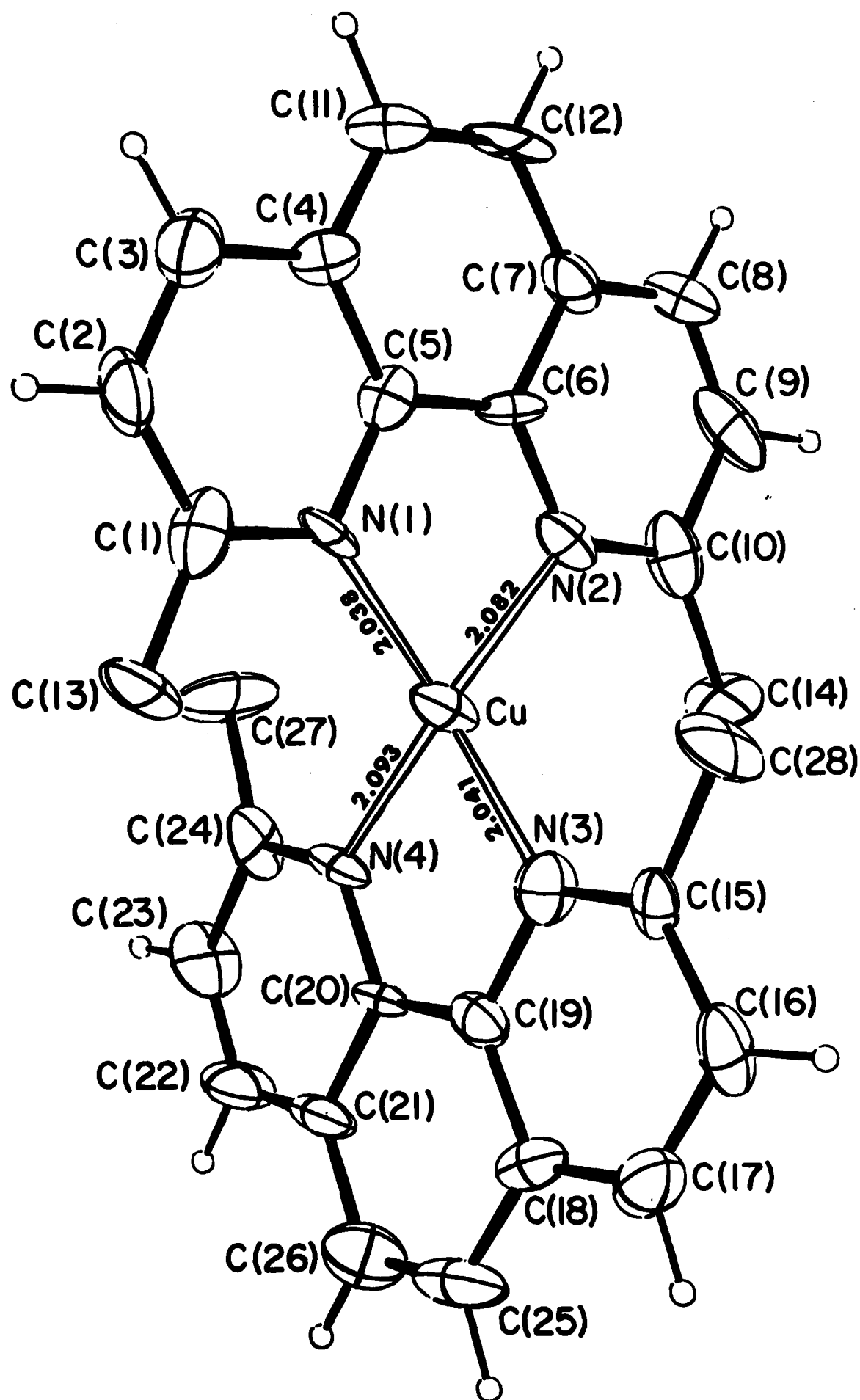
Figure 10. Temperature dependence of the integrated EPR spectral intensity for the triplet state fine structure lines ( $S = 1$ ) and the central line ( $S = 1/2$ ) as observed along the  $z$ -axis (filled circles) and  $x$ -axis (open circles) of the D-tensor. The solid lines are theoretical plots as discussed in the text.

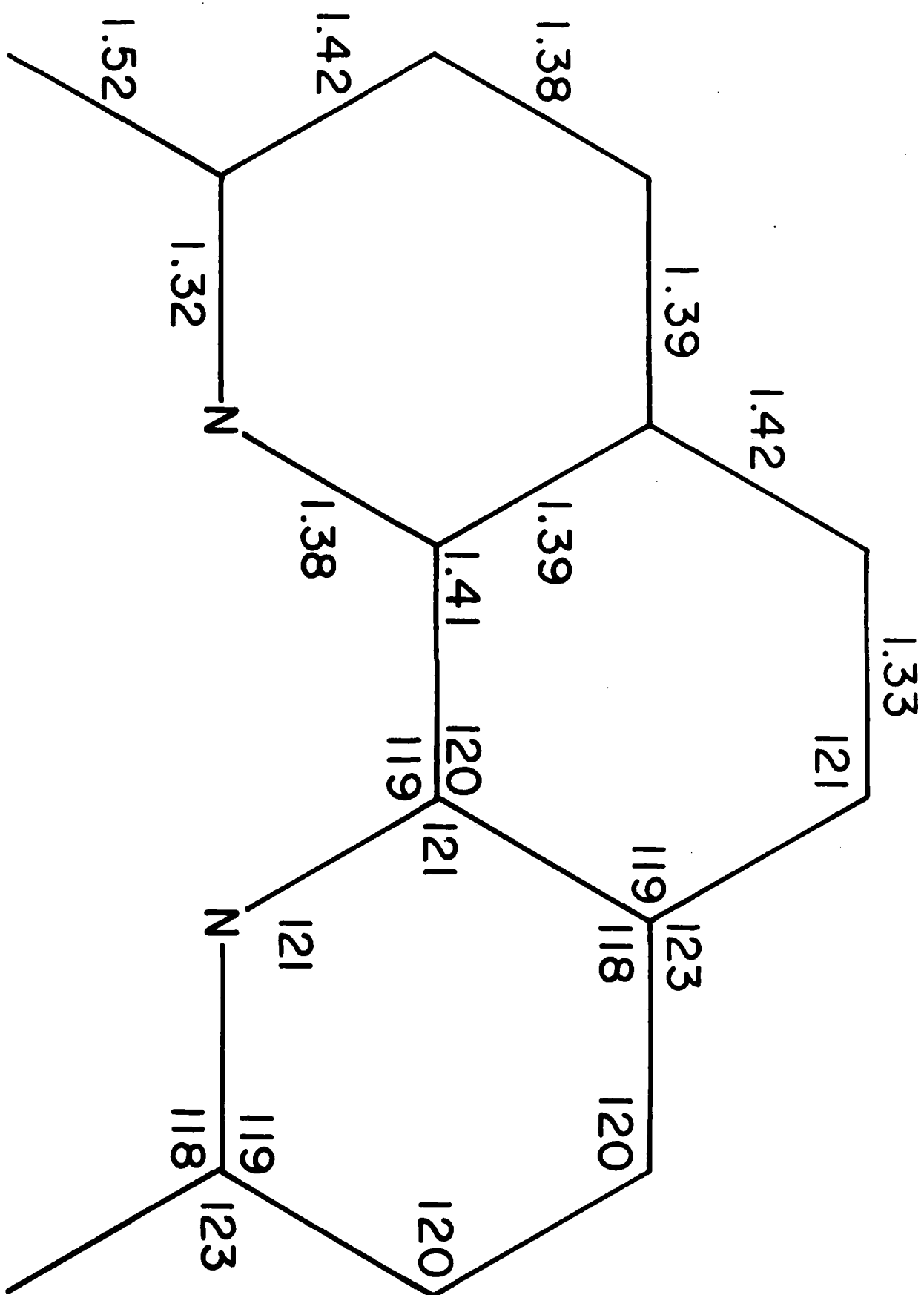
Figure 11. The ground and excited energy levels of the  $\sigma$ -bonded dianion a) for exchange coupled dimer, (b) for dipole-dipole coupled biradical.

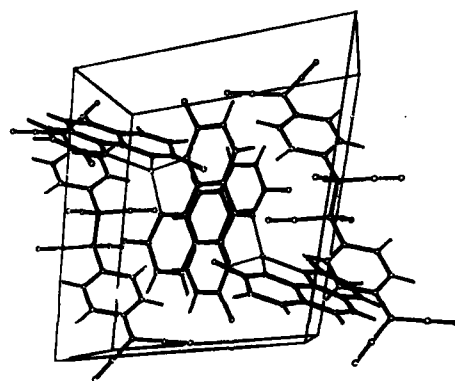
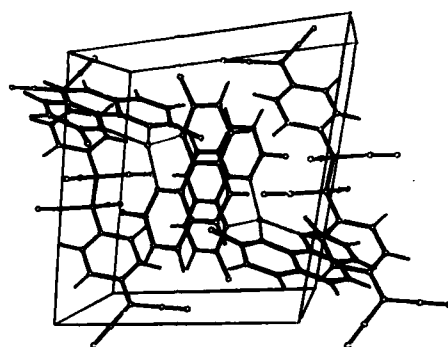
Figure 12. Relationship between the activation energy ( $E_a$ ) and fine structure parameter (D) for  $\sigma$ - and  $\pi$ -bonded TCNQ dimers, trimers, and tetramers. The data points are keyed by number to entries in Table VIII.



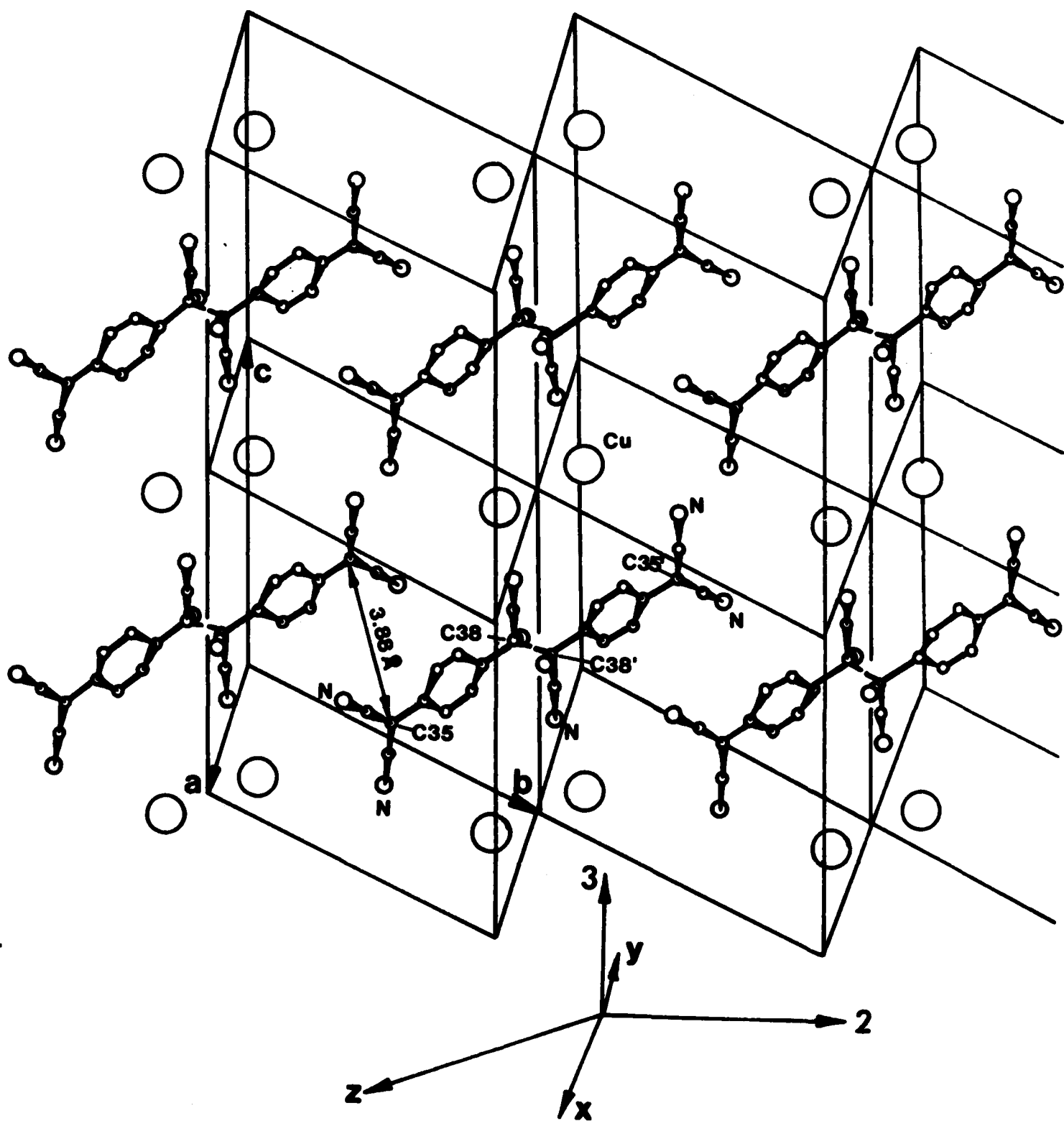




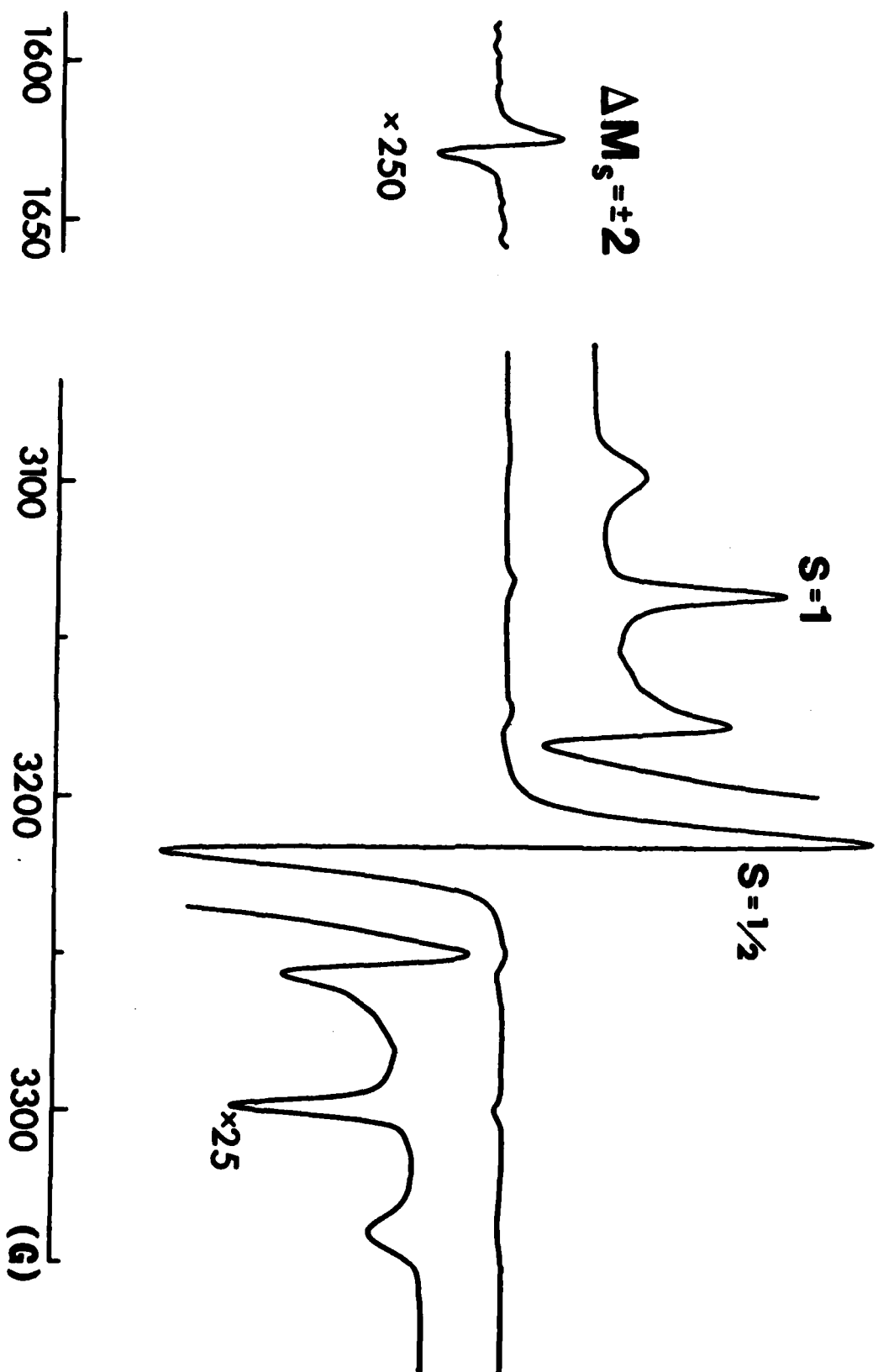


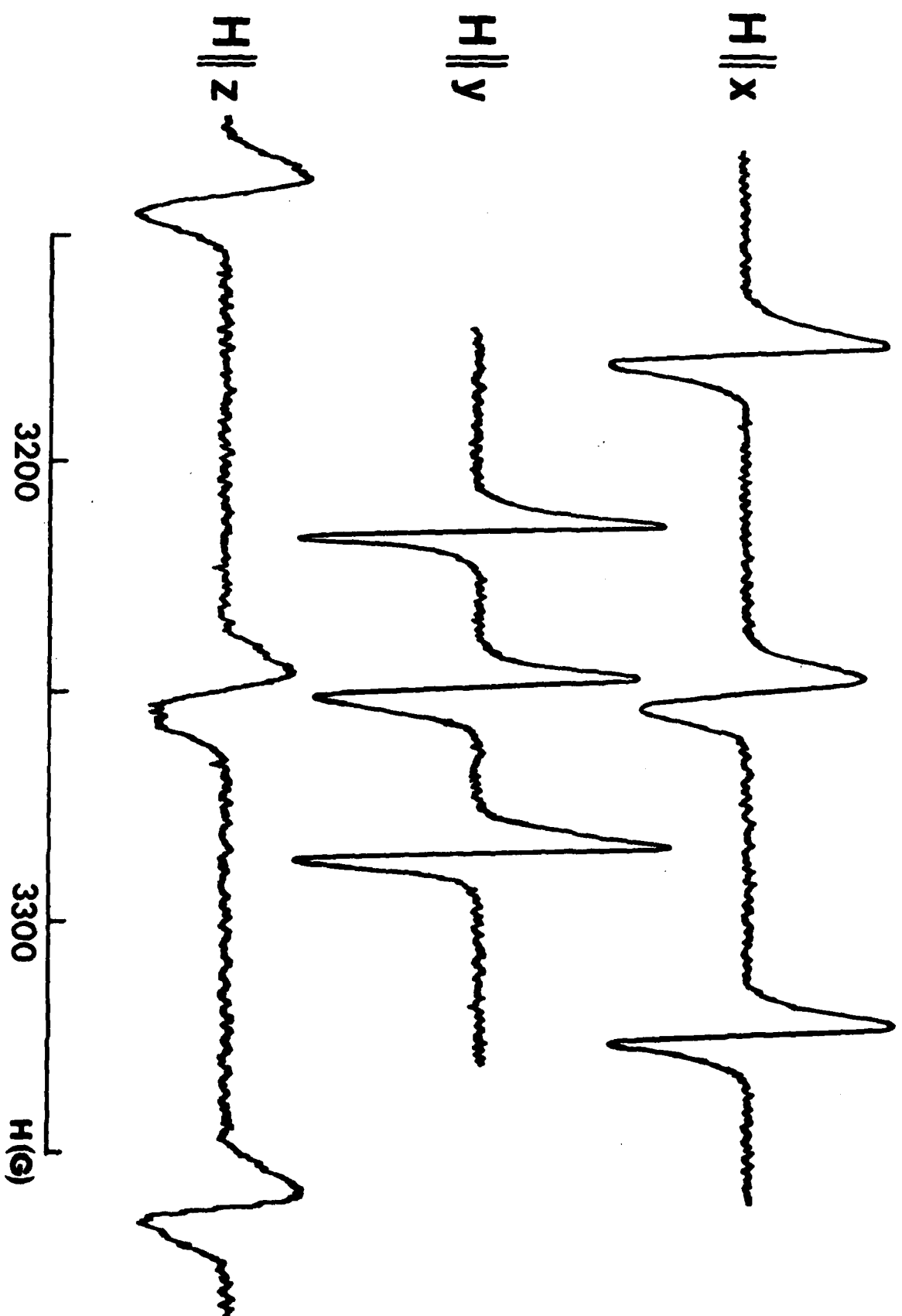


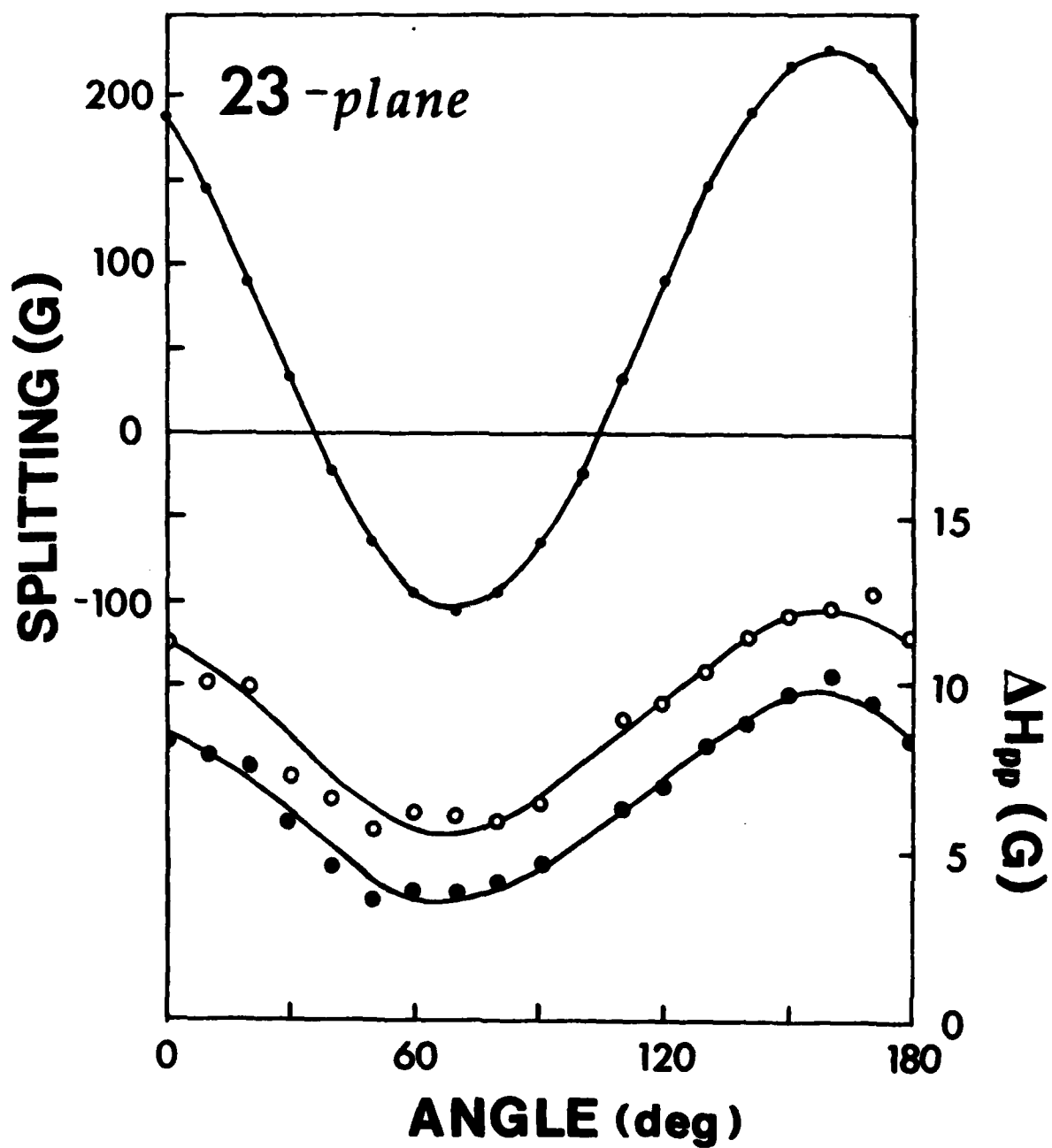


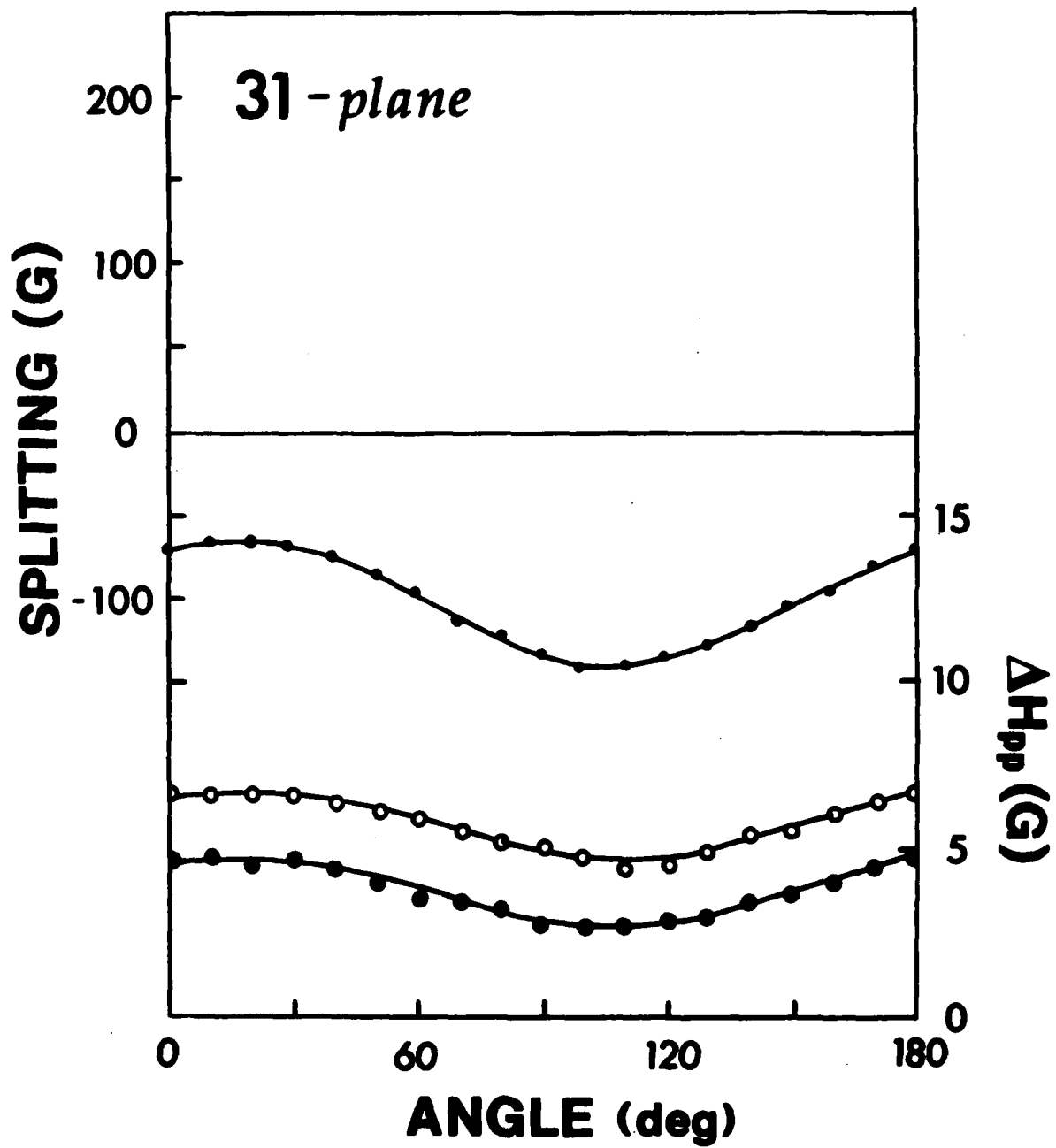


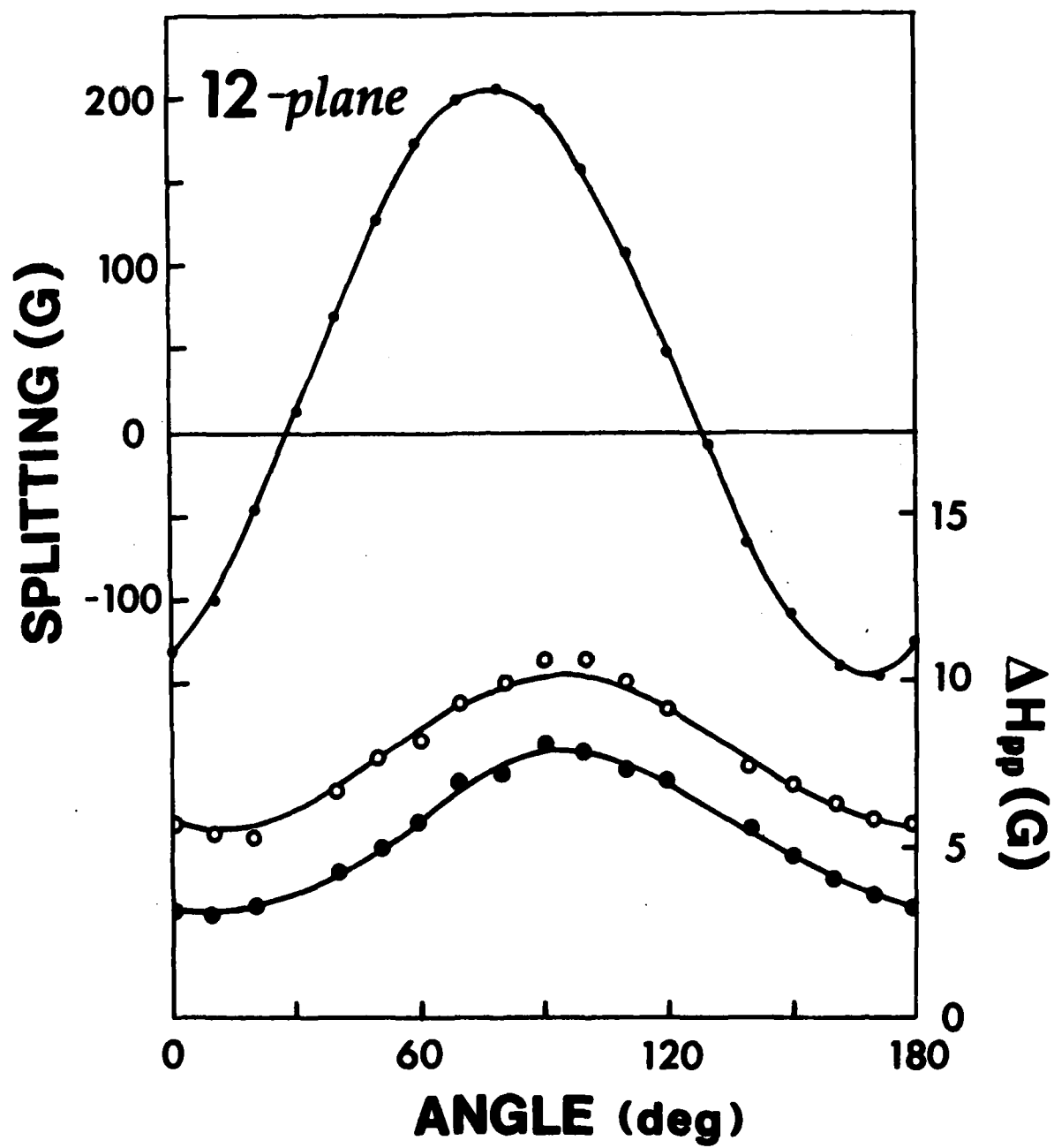
# $\text{Cu}(\text{DMP})_2\text{TCNQ}$

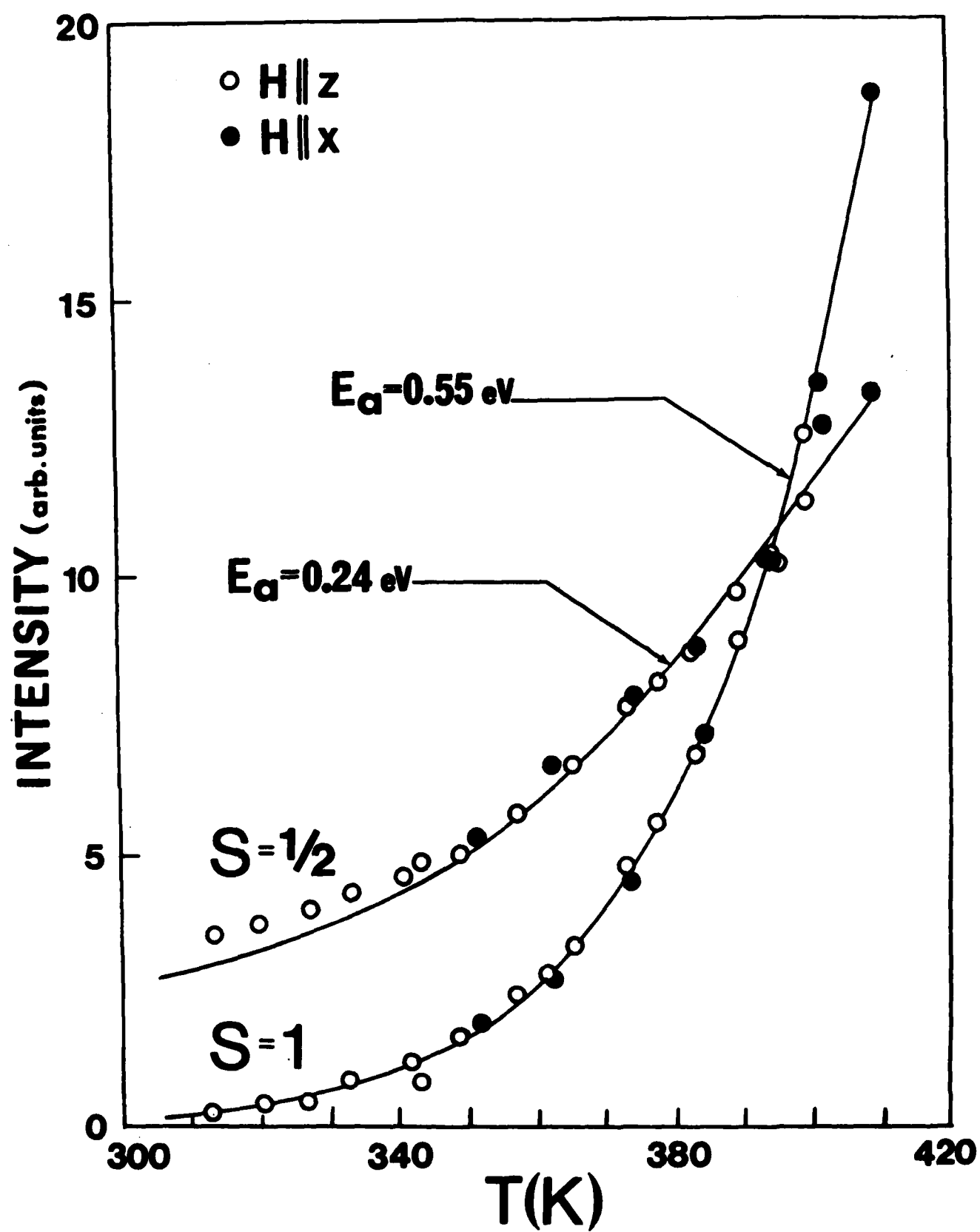


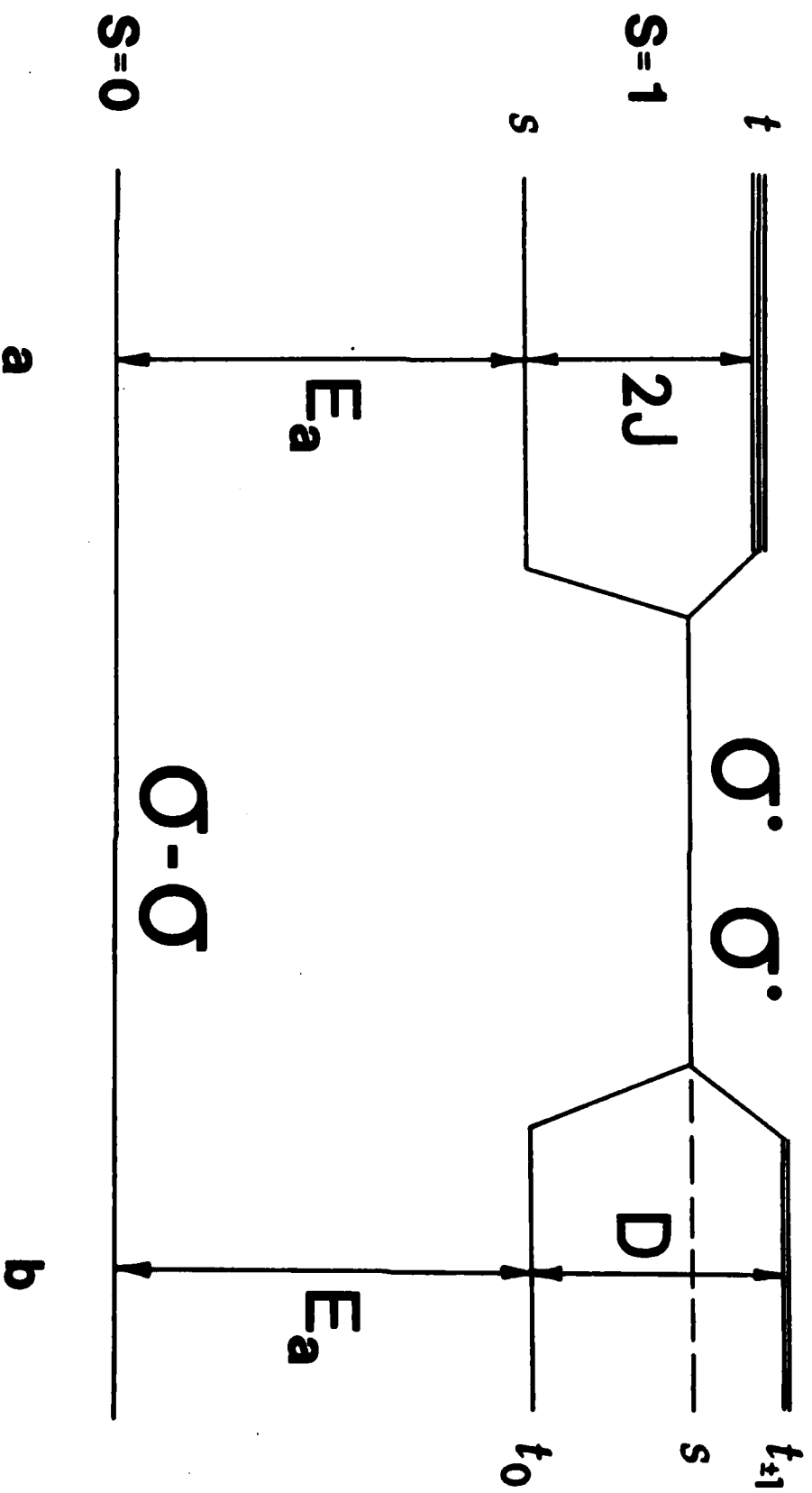




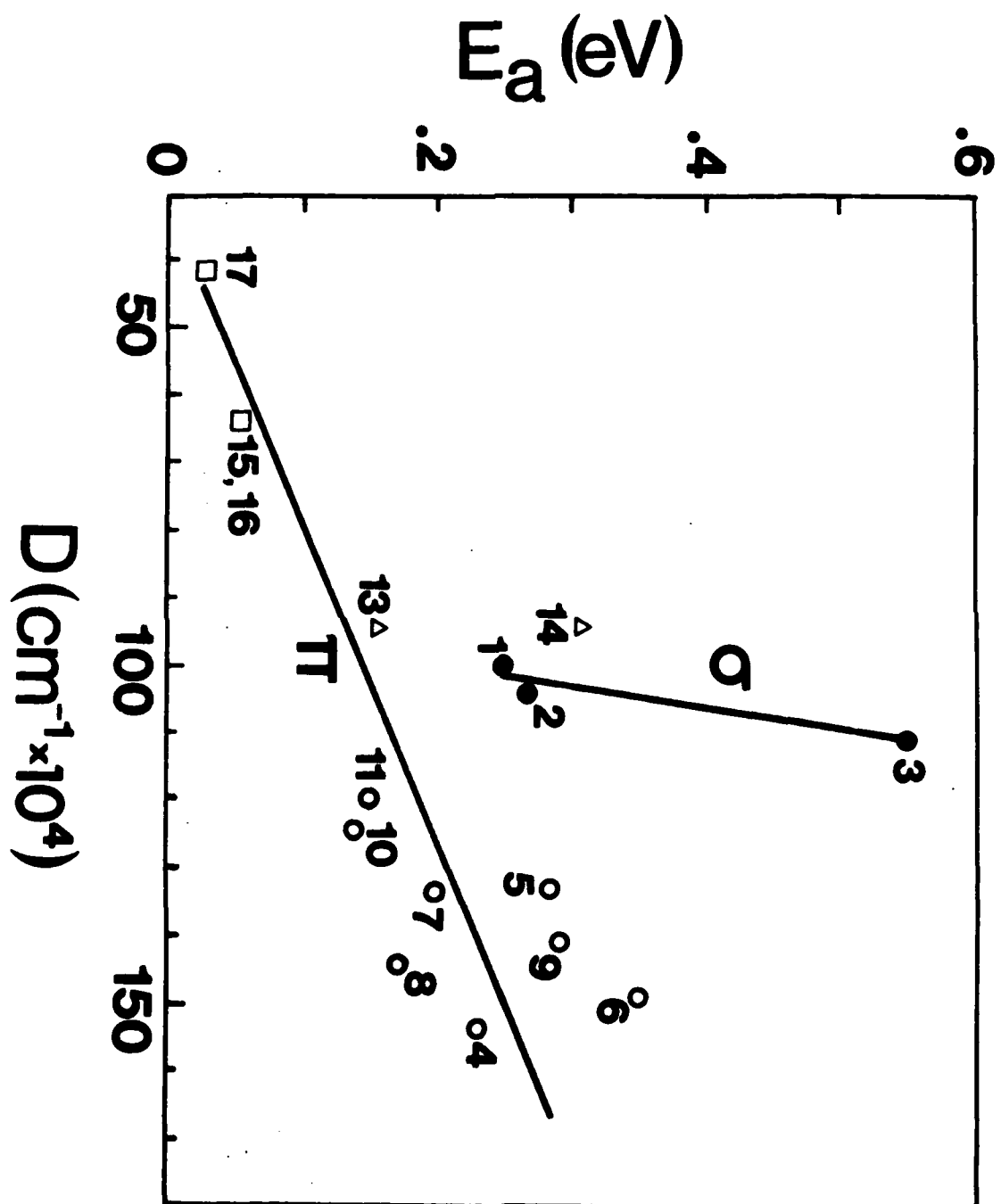












TECHNICAL REPORT DISTRIBUTION LIST, GEN

	<u>No. Copies</u>		<u>No. Copies</u>
Office of Naval Research Attn: Code 413 800 North Quincy Street Arlington, Virginia 22217	2	Naval Ocean Systems Center Attn: Mr. Joe McCartney San Diego, California 92152	1
ONR Pasadena Detachment Attn: Dr. R. J. Marcus 1030 East Green Street Pasadena, California 91106	1	Naval Weapons Center Attn: Dr. A. B. Amster, Chemistry Division China Lake, California 93555	1
Commander, Naval Air Systems Command Attn: Code 310C (H. Rosenwasser) Department of the Navy Washington, D.C. 20360	1	Naval Civil Engineering Laboratory Attn: Dr. R. W. Drisko Port Hueneme, California 93401	1
Defense Technical Information Center Building 5, Cameron Station Alexandria, Virginia 22314	12	Dean William Tolles Naval Postgraduate School Monterey, California 93940	1
Dr. Fred Saalfeld Chemistry Division, Code 6100 Naval Research Laboratory Washington, D.C. 20375	1	Scientific Advisor Commandant of the Marine Corps (Code RD-1) Washington, D.C. 20380	1
U.S. Army Research Office Attn: CRD-AA-IP P. O. Box 12211 Research Triangle Park, N.C. 27709	1	Naval Ship Research and Development Center Attn: Dr. G. Bosmajian, Applied Chemistry Division Annapolis, Maryland 21401	1
Mr. Vincent Schaper DTNSRDC Code 2803 Annapolis, Maryland 21402	1	Mr. John Boyle Materials Branch Naval Ship Engineering Center Philadelphia, Pennsylvania 19112	1
Naval Ocean Systems Center Attn: Dr. S. Yamamoto Marine Sciences Division San Diego, California 91232	1	Mr. A. M. Anzalone Administrative Librarian PLASTEC/ARRADCOM Bldg 3401 Dover, New Jersey 07801	1

TECHNICAL REPORT DISTRIBUTION LIST, 053

	<u>No. Copies</u>		<u>No. Copies</u>
Dr. M. F. Hawthorne Department of Chemistry University of California Los Angeles, California 90024	1	Dr. T. Marks Department of Chemistry Northwestern University Evanston, Illinois 60201	1
Dr. D. B. Brown Department of Chemistry University of Vermont Burlington, Vermont 05401	1	Dr. J. Zuckerman Department of Chemistry University of Oklahoma Norman, Oklahoma 73019	1
Dr. D. Venezky Chemistry Division Naval Research Laboratory Code 6130 Washington, D.C. 20375	1	Professor O. T. Beachley Department of Chemistry State University of New York Buffalo, New York 14214	1
Dr. John E. Jensen Hughes Research Laboratory 3011 Malibu Canyon Road Malibu, California 90265		Professor K. M. Nicholas Department of Chemistry Boston College Chestnut Hill, Massachusetts 02167	1
Dr. A. Cowley Department of Chemistry University of Texas Austin, Texas 78712	1	Professor R. Neilson Department of Chemistry Texas Christian University Fort Worth, Texas 76129	1
Dr. W. Hatfield Department of Chemistry University of North Carolina Chapel Hill, North Carolina 27514	1	Professor M. Newcomb Texas A&M University Department of Chemistry College Station, Texas 77843	1
Dr. M. H. Chisholm Department of Chemistry Indiana University Bloomington, Indiana 47401	1	Professor Richard Eisenberg Department of Chemistry University of Rochester Rochester, New York 14627	1
		Professor R. D. Archer University of Massachusetts Chemistry Department Amherst, Massachusetts 01003	